Crystals for heat-scintillation cryogenic bolometers used in the rare event searches

Matias Velazquez,[1] Philippe Veber,[2] Pierre de Marcillac,[3] Carmen Stelian,[2] Denys V. Poda,[3,6] Christophe Dujardin,[2] Abdelmounaim Ahmine,[1] Thierry Duffar,[1] Lydia Torres,[3] Andrea Giuliani,[3,4] Stefanos Marnieros,[3] Claudia Nones,[5] Valentina Novati,[3] Emiliano Olivieri,[3] I. Villa,[7] Anastasiia S. Zolotarova,[5] Thierry Redon[3]

[1]Univ. Grenoble Alpes, CNRS, Grenoble INP, SIMAP, 38000 Grenoble, France
[2]Université Lyon, Université Claude Bernard Lyon 1, CNRS, ILM UMR 5306, France
[3]IJCLab, Univ. Paris-Sud, CNRS/IN2P3, Université Paris-Saclay, 91405 Orsay, France
[4]DISAT, Università dell'Insubria, 22100 Como, Italy
[5]IRFU, CEA, Université Paris-Saclay, F-91191 Gif-sur-Yvette, France
[6]Institute for Nuclear Research, 03028 Kyiv, Ukraine
[7]Department of Material Science, University of Milano-Bicocca, Milano, Italy

http://clymene.in2p3.fr/

Bulk crystals for heat-scintillation cryogenic bolometers (HSCB) used in the rare events detection

- Cosmological observations show that baryonic matter, electrons, photons and neutrinos account for 6 % of the Universe energy content:

⇨ Attempts at detecting directly the neutralino, by means of several experiments based on several ~100 kg of single crystals detectors.

☞ *"First results on sub-GeV spin-dependent dark matter"*, A. H. Abdelhameed *et al.*, Eur. Phys. J. C, 79 (7) (2019) 630/1-7.

- Ultimate background noise in underground sites dedicated to the dark matter direct detection: fast neutrons ($\Psi \sim 10^{-6}$ n.cm^{-2}.s^{-1} for neutrons issued from the natural radioactivity of the mountain rocks and $\Psi \sim 10^{-9}$ n.cm^{-2}.s^{-1} for muon-induced neutrons)

- Neutrinoless double beta decays ($0\nu2\beta$) in ^{100}Mo-based crystals such as $ZnMoO_4$ or Li_2MoO_4

- Coherent elastic neutrino-nucleus scattering (CEνNS) detection

- Rare decays in specific isotopes (^{151}Eu, …)

- Solar axions detection (^{7}Li)

Bulk crystals for heat-scintillation cryogenic bolometers (HSCB) used in the rare events detection

- Cosmological observations show that baryonic matter, electrons, photons and neutrinos account for 6 % of the Universe energy content:

⇨ Attempts at detecting directly the neutralino, by means of several experiments based on several ~100 kg of single crystals detectors.

☞ *"First results on sub-GeV spin-dependent dark matter"* A. H. Abdelhameed *et al.*, Eur. Phys. J. C, 79 (7) (2019) 630/1-7.

LWMO crystals

- Ultimate background noise in undergro ... the dark matter direct detection: fast neutrons ($\Psi \sim 10^{-6}$ n.c ... sued from the natural radioactivity of the mountain rocks and Ψ ... on-induced neutrons)
- Neutrinoless double beta decays (0ν2β ... als such as ZnMoO ... or Li_2MoO_4
- **Coherent elastic neutrino-nucleus scattering (CEνNS) detection**
- Rare decays in specific isotopes (^{151}Eu, …)
- Solar axions detection (^{7}Li)

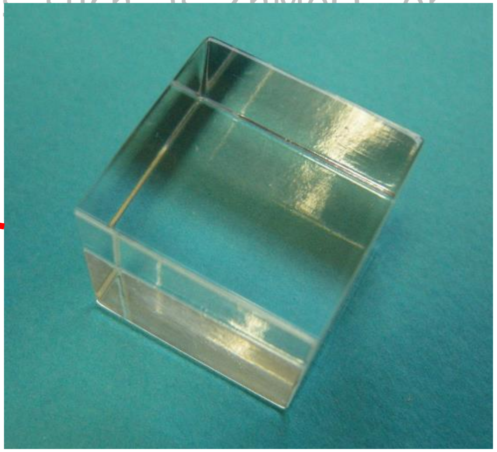

HSCB operation principle

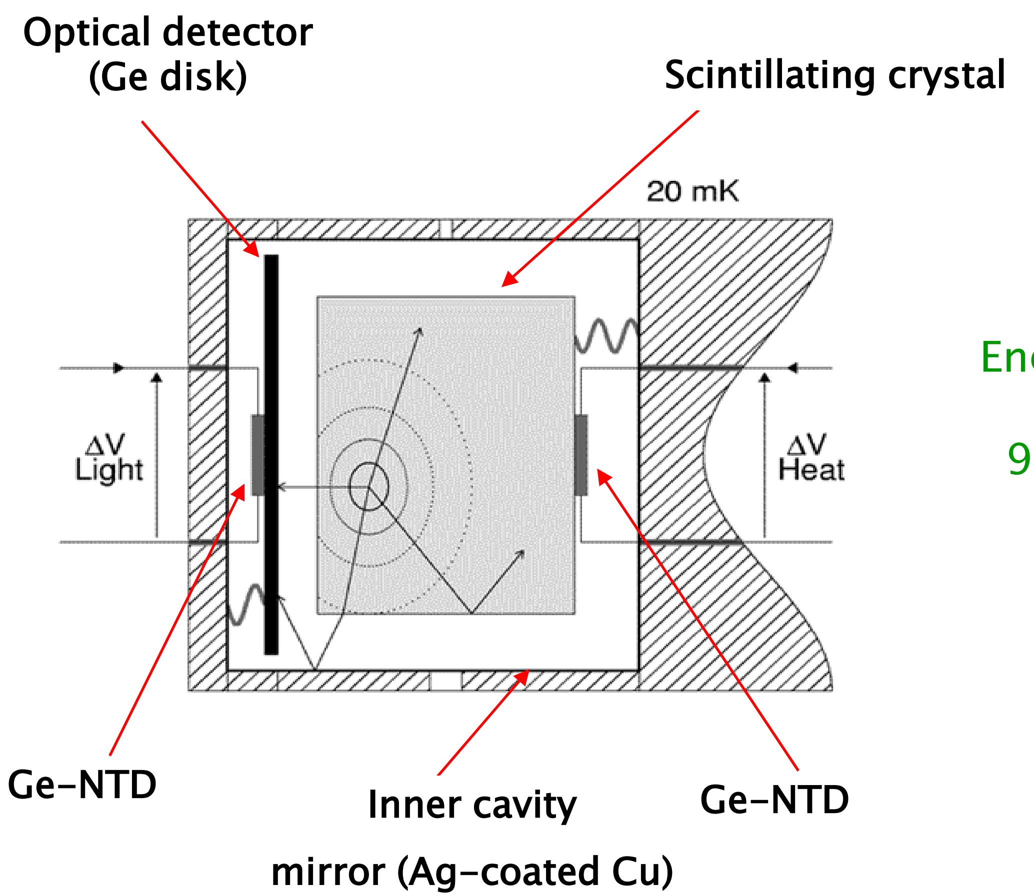

Energy conversion balance inside a LiF target:
90% heat, 3% light, 7% trapped

- C_p(10 mK) as low as possible; κ_{th}(10 mK) or θ_D as high as possible ;
- No thermoluminescence, sufficient emission between 400 and 1700 nm ;
- Isotopic concentrations ~10^{22} cm^{-3}, crystal masses 300 g to 1 kg.

HSCBs bulk crystals intended for fast neutrons spectroscopy
Collaboration with Pierre de Marcillac (IAS→CSNSM→IJCLab) since 2008

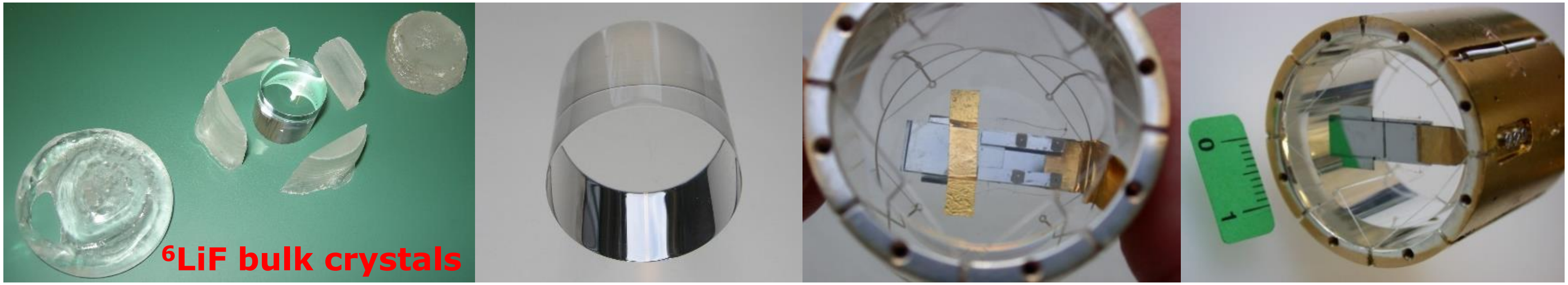

(Φ=2.5 cm, h=3.5 cm) 32 g ^{6}LiF crystals assembled in a HSCB detector at IAS-Orsay (front face view, optical bolometer side/the sensor and the thermal leak are seen behinf the transparent cylinder).

Probably one of the first, in 2011, fast neutrons spectrometer in the world to be so compact, with an energy resolution ~50 keV FWHM on thermal neutrons. But also a complex prototype : - second (very long) time constant (600 ms, not of radiocontamination origin but likely to be due to extended defects) ; - light yields **0.12 keV/MeV** on $\mu/\beta/\gamma$, **0.033** keV/MeV on α and **0.041** keV/MeV on α+tritium, making possible discrimination from 2 to 10 MeV between fast and thermal neutrons and $\mu/\beta/\gamma$'s, but not sufficiently from α's.

Aboveground, 20 mK

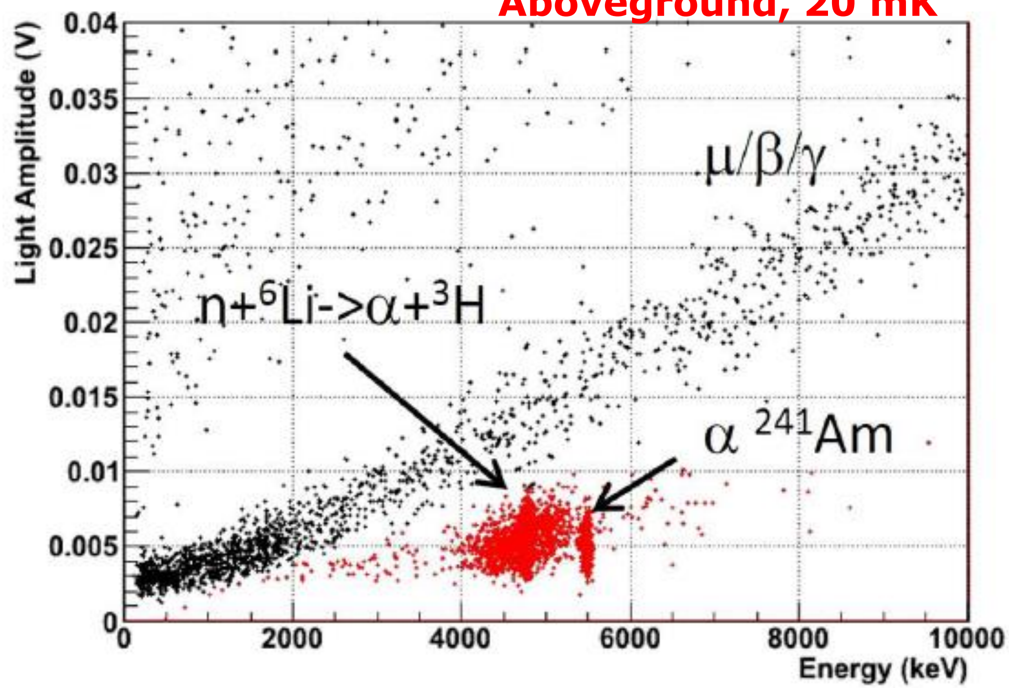

HSCBs bulk crystals intended for fast neutrons spectroscopy (2)
Collaboration with Pierre de Marcillac (IAS→CSNSM→IJCLab) since 2008

Table 1. Most used neutron-induced reactions for fast neutron spectroscopy.

Reaction (energy at thermal capture)	Q_{value} (MeV)	σ (E_n=1 MeV) (barns)
n+^{3}He→^{3}H (0.191 MeV) + p (0.574 MeV)	0.765	0.7
n+^{6}Li→α (2.050 MeV) + ^{3}H (2.730 MeV)	4.783	0.3
n+^{10}B→^{7}Li (1.015 MeV) + α (1.777 MeV) (6%) n+^{10}B→^{7}Li* (0.840 MeV) + α (1.470 MeV) (94%) ↪^{7}Li + γ (0.48 MeV)	2.792	0.04

Thermoluminescence issues in ^{6}LiF led us to grow multitarget rare earth lithium borates, which contain ^{6}Li, $^{155/157}$Gd, ^{10}B isotopes and allow for tuning the composition.

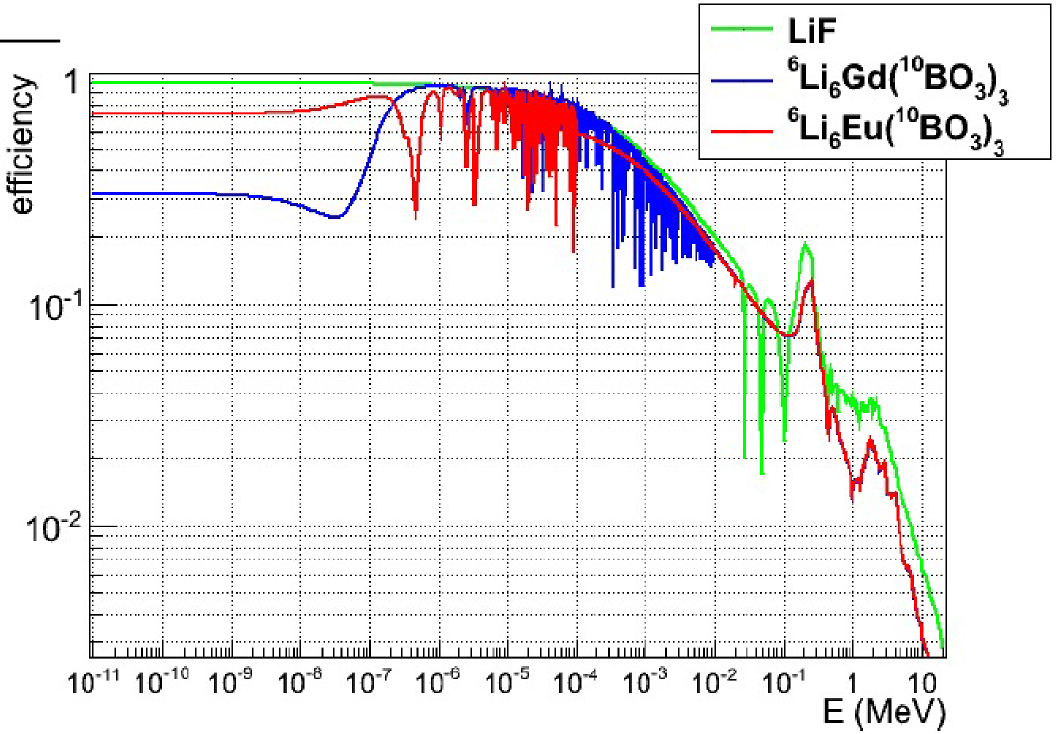

Figure 1. Calculated efficiency of ^{6}LiF, $^6Li_6Gd(^{10}BO_3)_3$ and $^6Li_6Eu(^{10}BO_3)_3$ (800 gr, cylindrical shape (h=ϕ), 95% enrichments).

M. Martínez *et al., (TAUP 12, Munich, september 2011), J. Phys.: Conf. Series, 375 (2012) 012025, 1-4.*

HSCBs bulk crystals intended for fast neutrons spectroscopy (3)
Collaboration with Pierre de Marcillac (IAS→CSNSM→IJCLab) since 2008

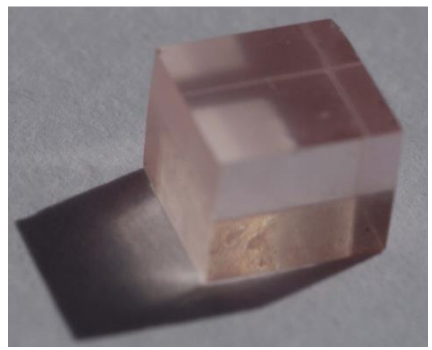

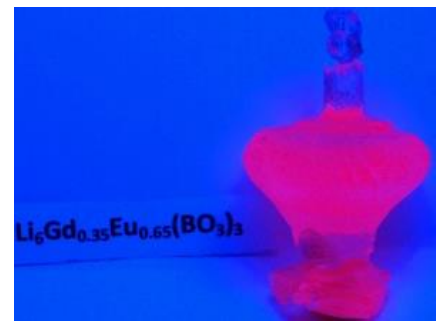

30 g

43.5 g et 17.7 g

Excitation 365 nm

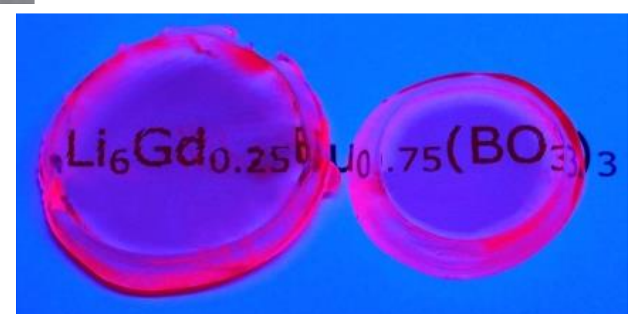

e=6 mm

ϕ=30 mm et 23 mm

HSCBs bulk crystals intended for fast neutrons spectroscopy (4)
Collaboration with Pierre de Marcillac (IAS→CSNSM→IJCLab) since 2008

- Light yields in LEB crystals 10 times more scintillating than LiF
- FWHM resolution 13 keV in LEB crystals on ^{10}B neutron capture reaction @2.31 MeV
- Three reactions well separated

$Li_6Eu(BO_3)_3$

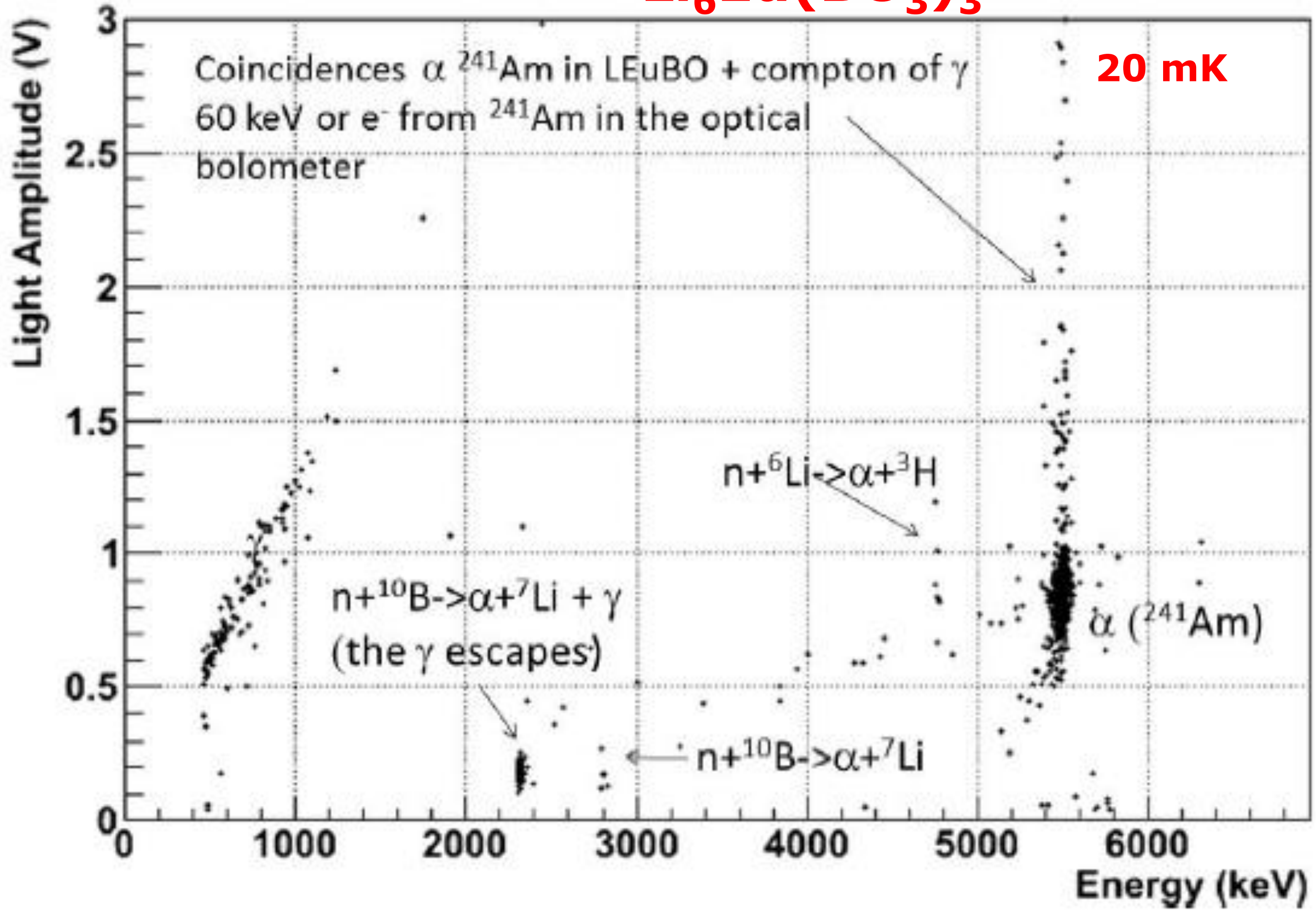

M. Martínez *et al.*, *(TAUP 12, Munich, september 2011), J. Phys.: Conf. Series, 375 (2012) 012025, 1–4.*

HSCBs bulk crystals used in (neutrino) astroparticle physics

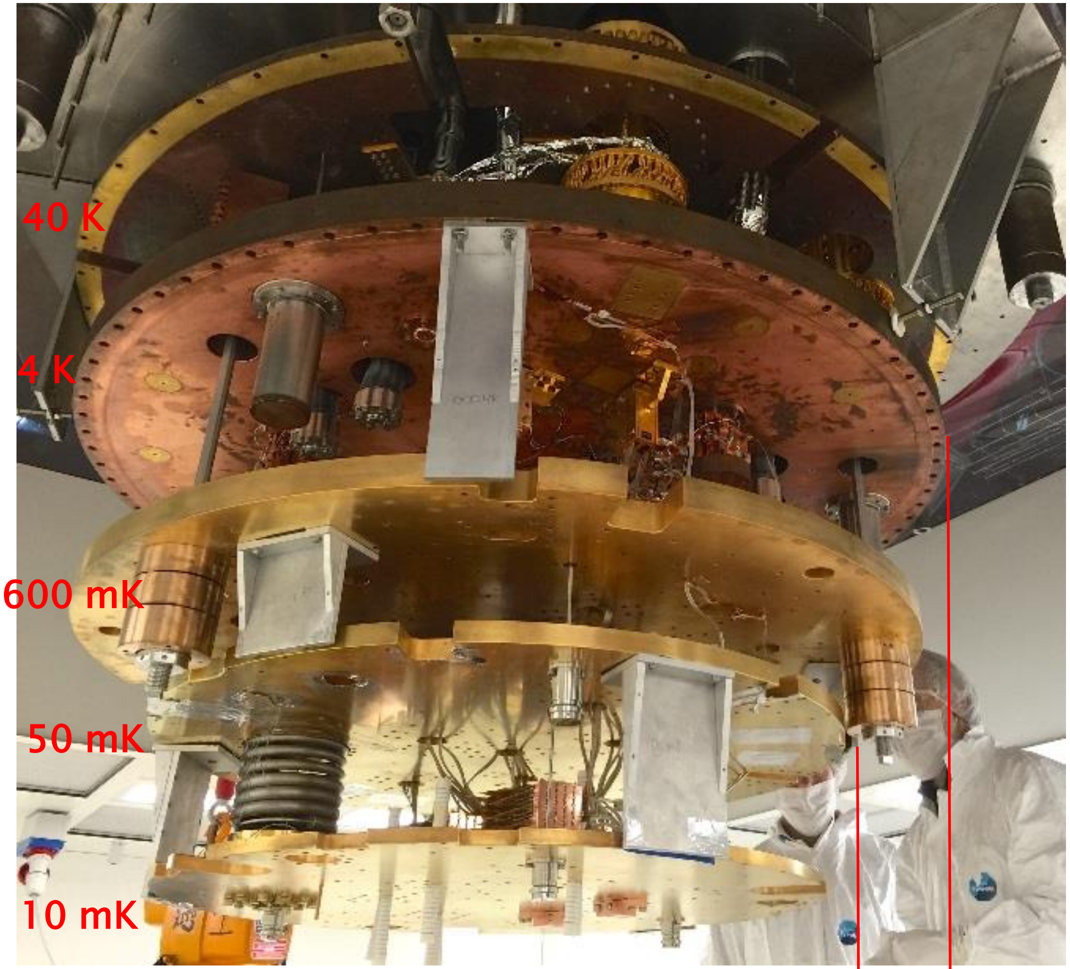

Construction 2007-2016
Measuring 2016-2021

15 t

3 t
(Pb, Cu, TeO_2)
Cooling 1.5 month

National Institute of Nuclear Physics
LNGS Gran Sasso National Laboratory
INFN

CUORE experiment

19 towers of 13 floors containing each 4 TeO_2 crystals of 742 g (206 kg of ^{130}Te)

« The coldest m³ known in the Universe … during 15 days »

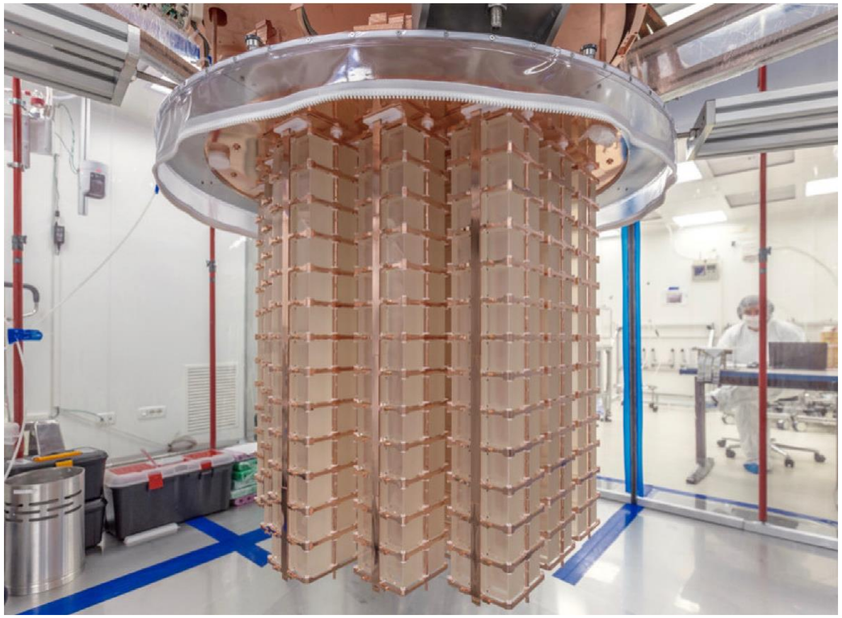

CUPID Detector

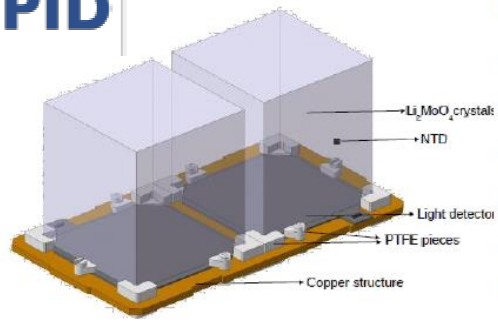

Single Detector

$Li_2{}^{100}MoO4$, 45x45x45 mm, 280 g

Ge light detector as in CUPID-Mo, CUPID-0

Gravity stacked structure
Crystals thermally interconnected

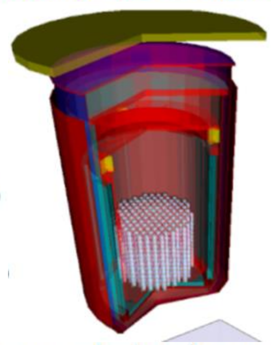

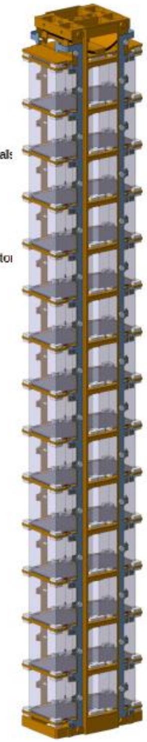

Tower

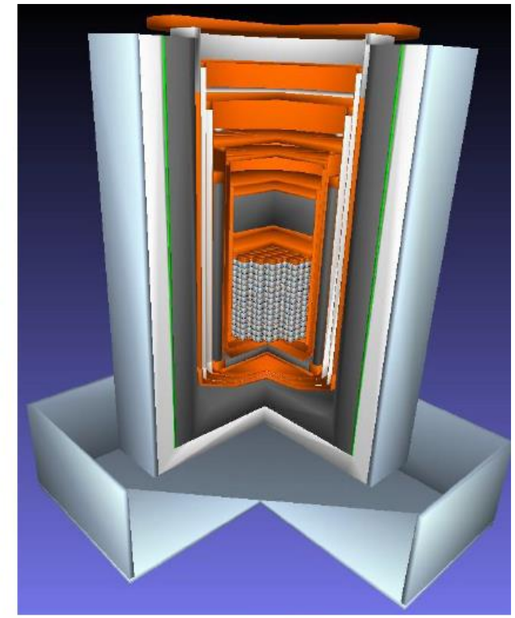

Detector Array

~240 kg of ^{100}Mo with >95% enrichment

~1.6.10^{27} ^{100}Mo atoms

57 towers of 14 floors with 2 crystals each, 1596 crystals

Tower Arrangement

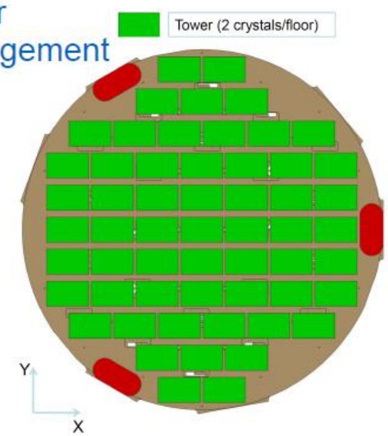

Opportunity to deploy multiple isotopes, phased deployment

K. Heeger and M. Pavan North America - Europe Workshop on Future of Double Beta Decay 29 September – 1 October 2021

- CUPID's objective is to replace non scintillating $^{130}TeO_2$ crystals by 1596 $Li_2{}^{100}MoO_4$ crystals ~280 g each, between 2023 and 2027.

Bulk LMO crystal growth in the literature

- Vertical Bridgman technique in a three-zone furnace : colored crystals, polluted by inclusions and cracked (P. Chen *et al.*, Materials Letters. 215 (2018), 225-228 & J. Crystal Growth. 500 (2018), 80-84) ;

- Growth from aqueous solution, with strong acoustic mixing in order to destroy the oxide clusters occurring in the liquid: this technique shows a great potential, but only millimetric crystals have been grown so far (O. P. Barinova *et al.*, Glass and Ceramics. 72 (2015), 11-12) ;

- The Czochralski technique was used for the growth of the very first single crystals in the '70s (I. D. Tretyak *et al.*, Kristallografiya. 19 (1974), 876-877). This process has been further developed, from crystals 34 g (O. P. Barinova *et al.*, Nuclear Instruments and Methods in Physics Research A, 607 (2009), 573-575) in weight to more than 700 g (V. Grigorieva *et al.*, J. Materials Science and Engineering. B 7 (2017), 63-70) ;

- This research effort eventually led to the Low Temperature Gradient Czochralski (LTG-Cz) technique, which is now the reference process for the growth of Li_2MoO_4 scintillating crystals. However, this technique has low growth rate ($\leq$ 0.7 mm.h^{-1}).

Outline

- Growth of Li_2MoO_4 (LMO) crystals by the unoptimized Czochralski method/Crack formation and characterization
- Modelling and numerical simulation of the LMO crystals Czochralski growth
- Bolometric operation with and without crystal fracture
- Absorption and scintillation emission properties of LMO crystals
- Optimized Czochralski growth of LMO crystals, thermo-mechanical properties characterizations and re-investigation of the thermal stresses

Conclusions and perspectives

Czochralski pulling of a Li_2MoO_4 crystal for the 0ν2β decay searches

- h=6 cm, ϕ_{ave}=4 cm
- Total mass =230.54 g
- Crystallization yield = 56 %
- Colourless cristal
- No cleavage nor facets (low Jackson factor)

GROWN UNDER MANUAL CONTROL

- Congruent melting at ≈702 °C
- Pt crucible in air
- Single crystalline [110]-oriented LMO seed
- Low pulling and rotation rates (0.6 mm/h and 5 rpm, average mass uptake rate ~3.5 g/h)
- Cooling rate 3.7°C/h

Crack formation at the bottom part of the bulk crystal

Crack orientation in a Li_2MoO_4 crystal/Simplified drawings of the crystal structure

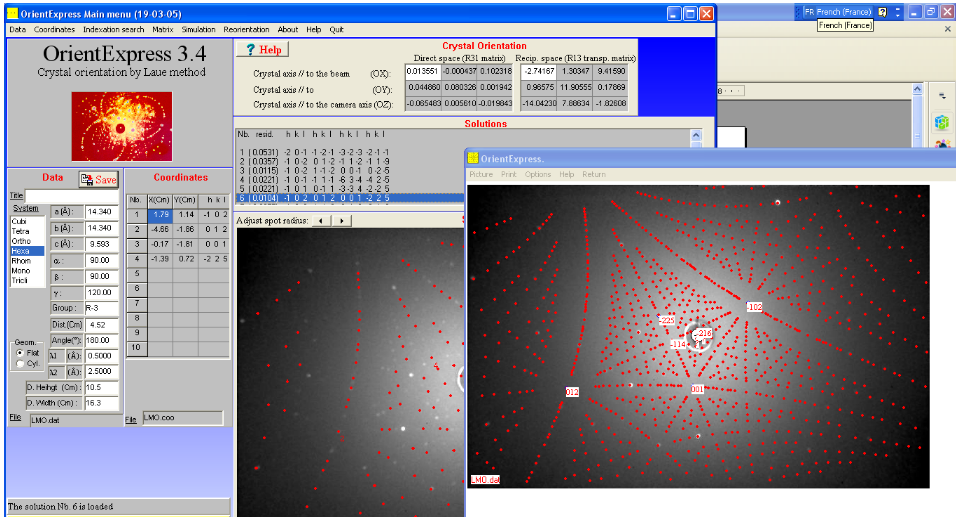

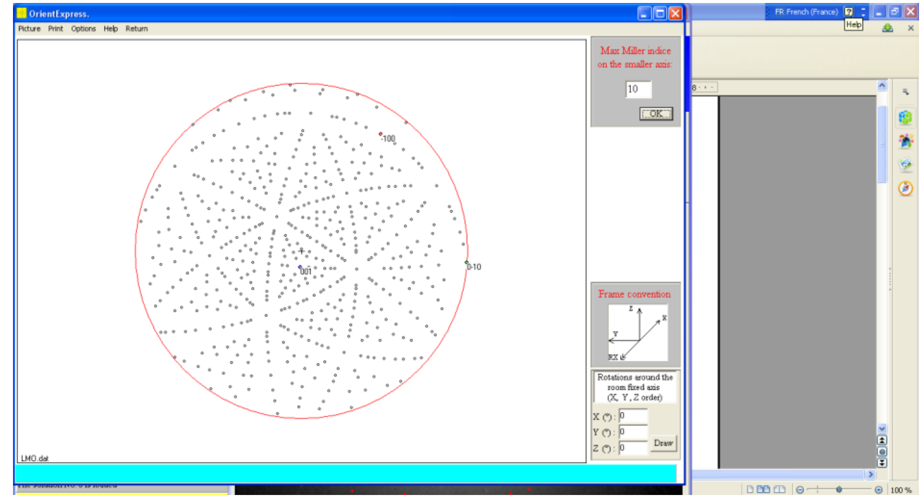

The only (cutting-induced) crack observed to date is oriented ≈11°Φ_Y and ≈1.1°Φ_Z away from (001) planes

R -3, a=b=14.34 Å, c=9.593 Å, γ=120°

Growth direction ~[110]

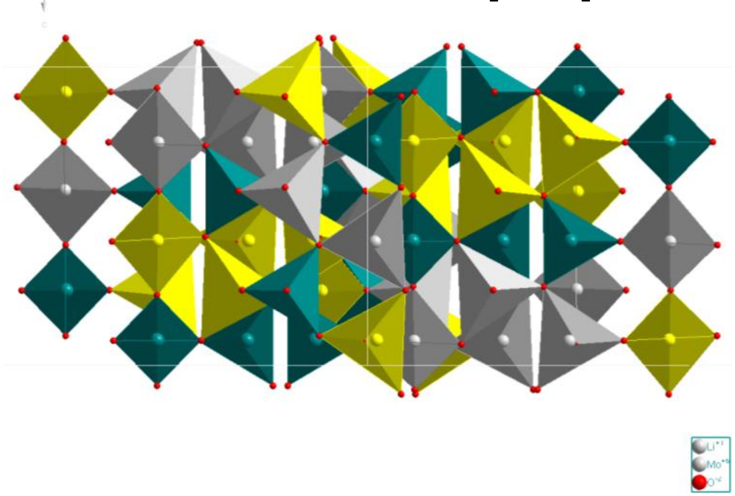

[001]-direction

(001) planes are less dense

$d_{[001]}$=c≈9.6 Å

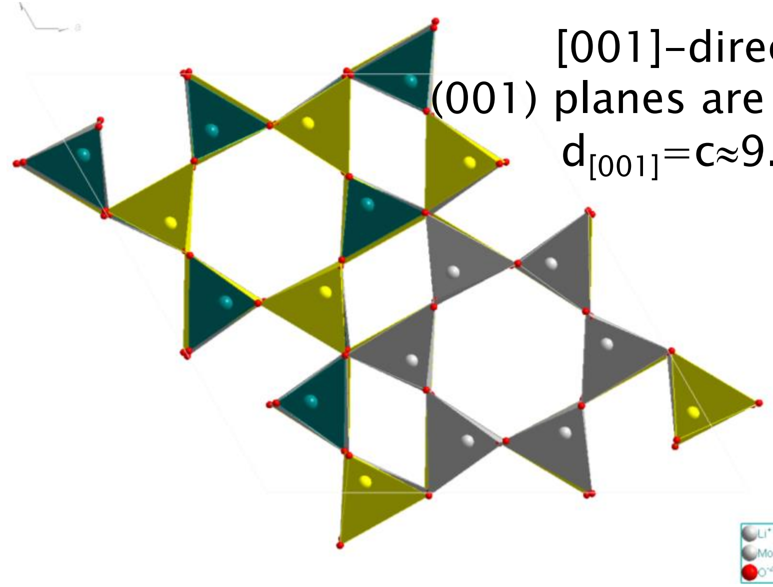

Outline

- Growth of Li_2MoO_4 (LMO) crystals by the unoptimized Czochralski method/Crack formation and characterization
- Modelling and numerical simulation of the LMO crystals Czochralski growth
- Bolometric operation with and without crystal fracture
- Absorption and scintillation emission properties of LMO crystals
- Optimized Czochralski growth of LMO crystals, thermo-mechanical properties characterizations and re-investigation of the thermal stresses

Conclusions and perspectives

Finite element 2D ½ modelling of the Czochralski pulling process of the ICMCB laboratory (COMSOL Multiphysics)

☞ Conservation equations:

- Mass conservation equation

$$\rho \nabla \vec{u} = 0$$

- Navier-Stokes equation

$$\rho[\frac{\partial \vec{u}}{\partial t} + (\vec{u}\nabla)\vec{u}] = -\nabla p + \mu \nabla^2 \vec{u} + \rho \vec{g}[1 - \beta_T (T - T_f)]$$

- Heat conservation equation

$$\rho c_P (\frac{\partial T}{\partial t} + \vec{u} \nabla T) = k \nabla^2 T + Q_R$$

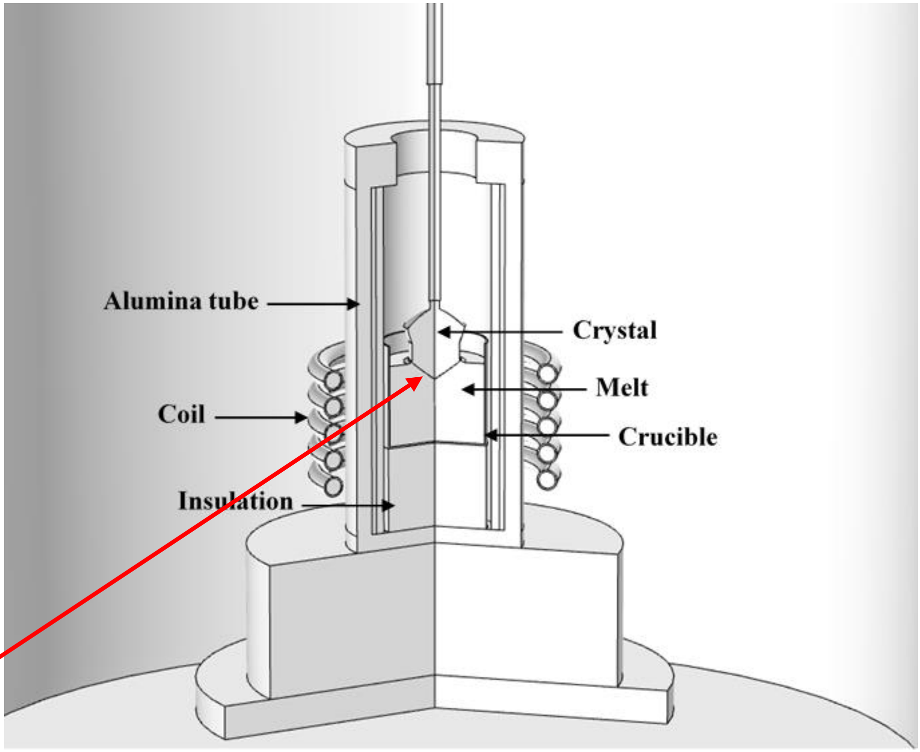

☞ At the liquid-solid interface:

$$\lambda_L \nabla T_L + \rho \Delta H.V = \lambda_S \nabla T_S$$

☞ Internal radiative contribution of the (semi-transparent) cristal to thermal transfer treated in the P1 approximation ($Q_R = a[G - 4n^2\sigma_B T^4]$) ;

☞ Rosseland formula : $k_S^{eff} = k_S + \frac{16 n^2 \sigma T^3}{3a}$, $\kappa_s^{eff}/\kappa_s \approx 150$

Numerical simulation of a Ø=3 cm LMO crystal pulling

Experimental observation of the solidification interface shape by quick extraction at different crystal pulling distances

Solidified distance = 3.2 cm
V=0.5 mm/h
ω=5 rpm

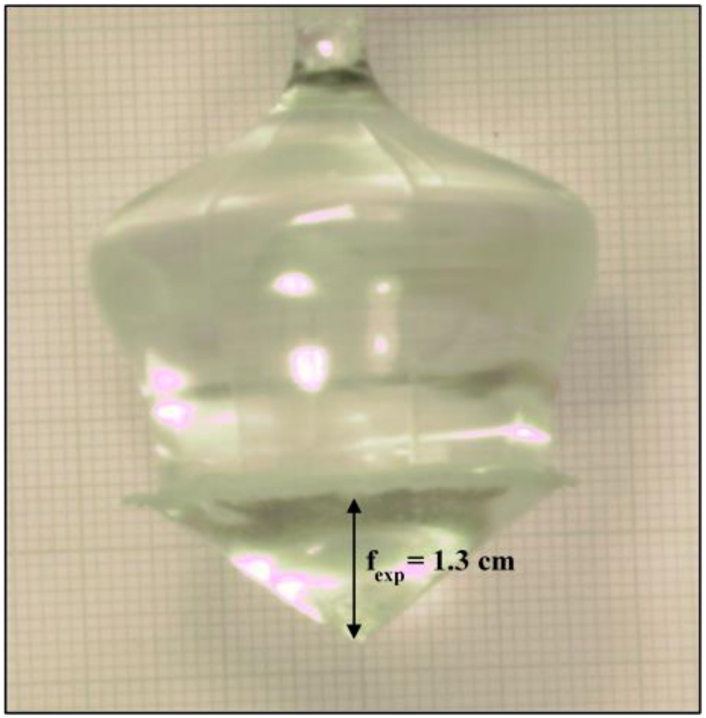

- Interface deflection =1.3 cm

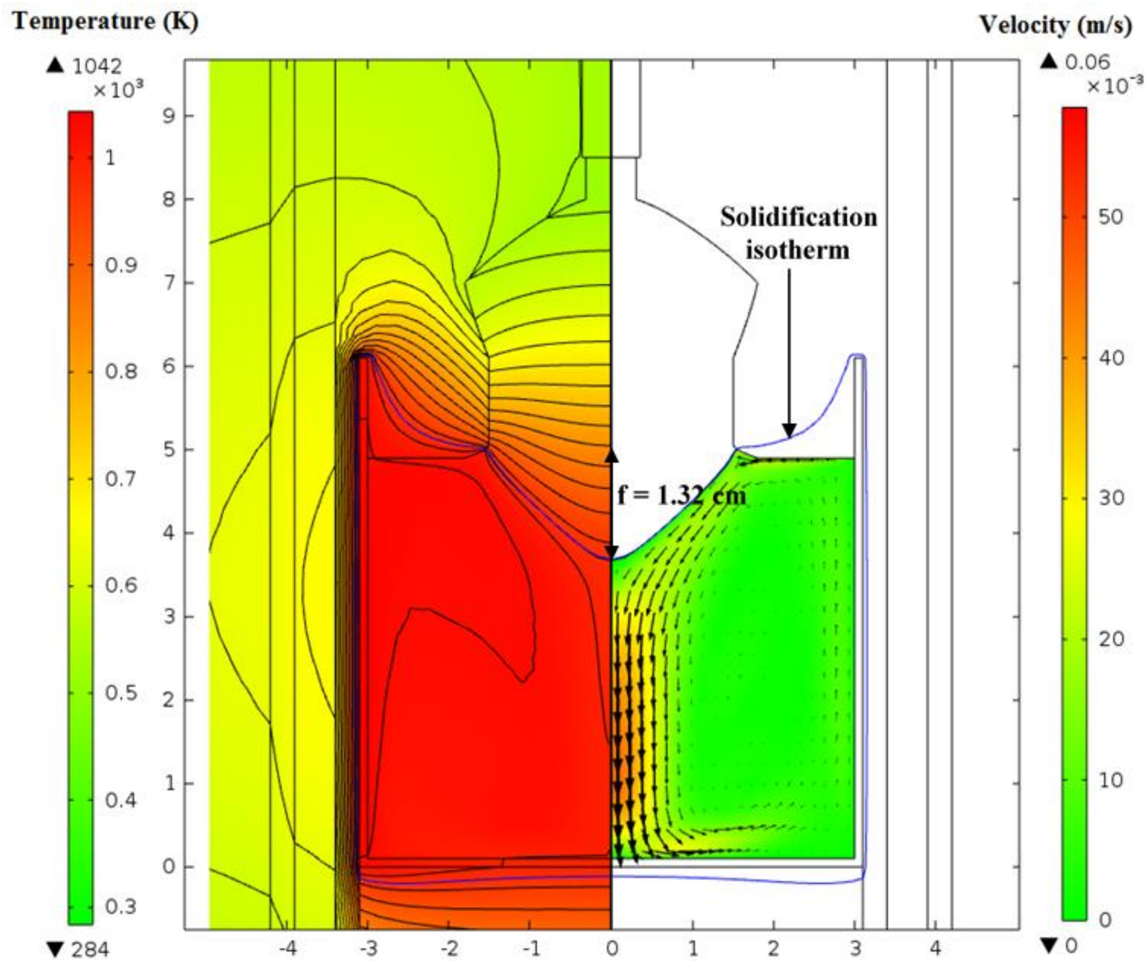

- Interface deflection =1.32 cm

Stelian *et al.*, J. Cryst. Growth, 492 (2018) 6-12

Numerical simulation of a Ø=3 cm LMO crystal pulling (2)

Solidified distance =5-6 cm
v=0.5 mm/h
ω=5 rpm

Experimental confirmations of:

- the convection vortices rotation direction ;
- the heat power ;
- the instability of this configuration ;
- the upward movement of the solidification isotherm in the bottom of the crucible and related mass uptake acceleration ;
- the solidification interface shape ;
- the instability induced by an increase in ω .

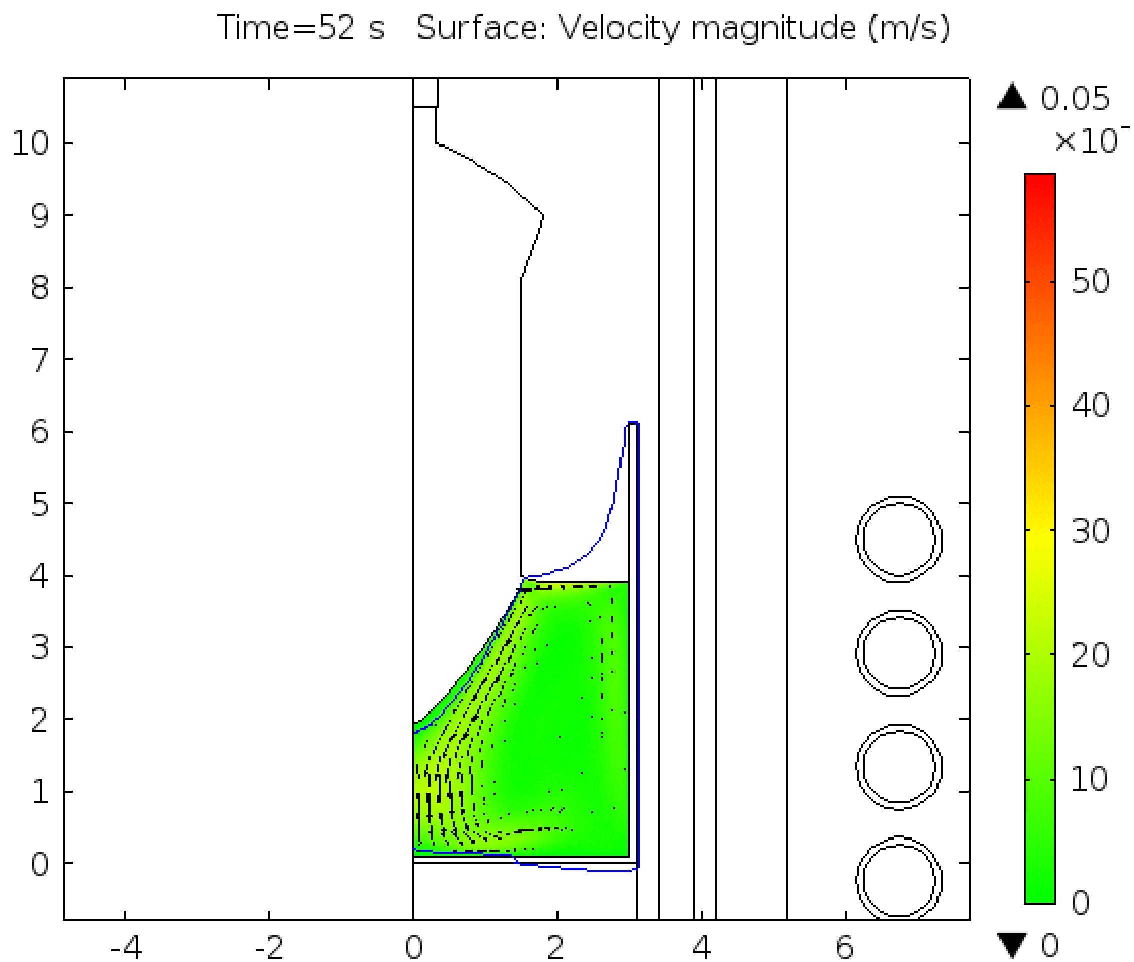

- Interface deflection =1.95 cm

Numerical computations of the Von Mises stress in LMO crystal

Numerical results for a 4 cm diameter crystal at solidified distance 6 cm

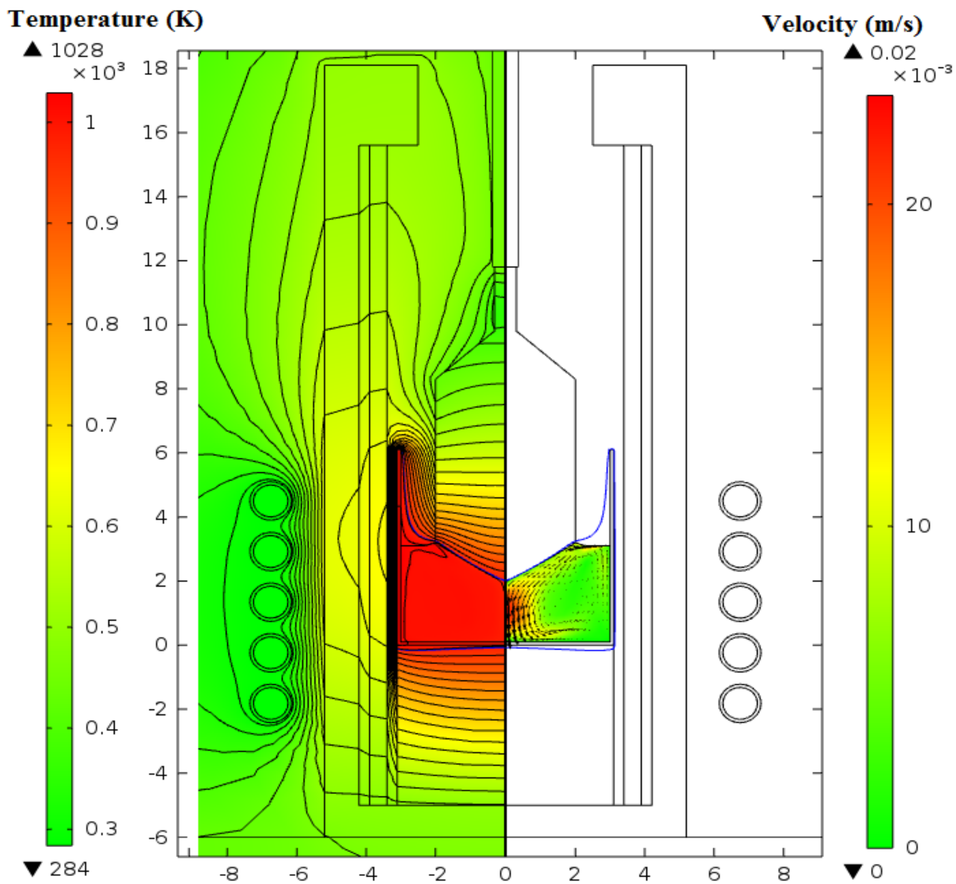

- Generalized Hooke's law $\sigma_{ij} = C_{ijkl}\left[\varepsilon_{kl} - \alpha_{kl}\left(T - T_{ref}\right)\right]$
- $\sigma_{Mises} = \sqrt{\dfrac{(\sigma_{xx}-\sigma_{yy})^2+(\sigma_{yy}-\sigma_{zz})^2+(\sigma_{zz}-\sigma_{xx})^2+6(\sigma_{xy}^2+\sigma_{yz}^2+\sigma_{xz}^2)}{2}}$.

Numerical computations of the Von Mises stress in LMO crystal (2)

Numerical results for a 4 cm diameter crystal at solidified distance 6.3 cm

Convex shape of the crystal tail

Temperatures and velocities

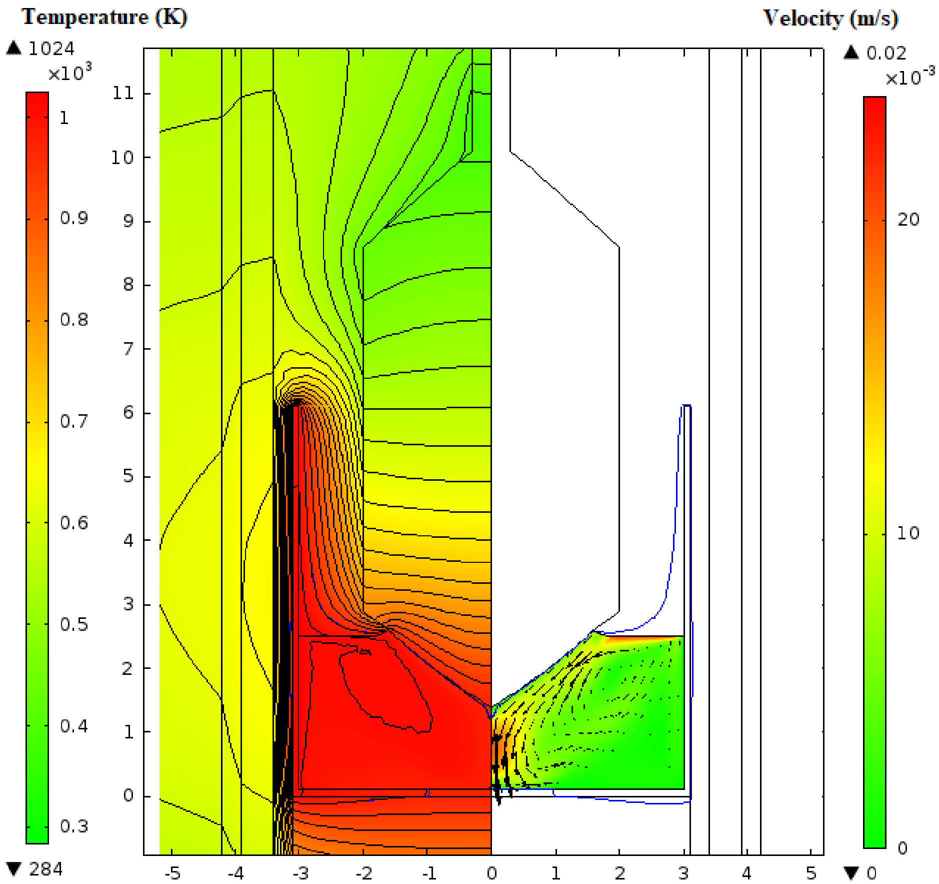

Von Mises stress

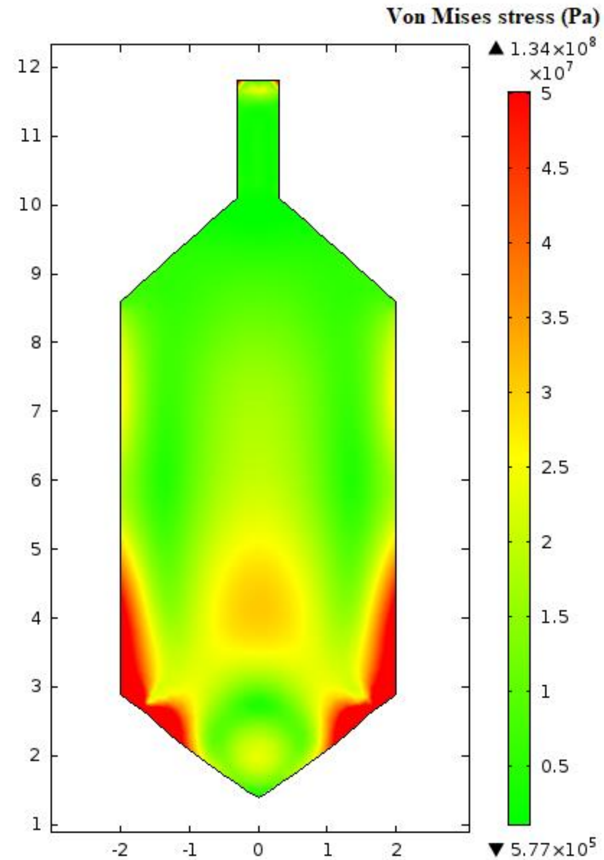

Numerical computations of the Von Mises stress in LMO crystal (3)

Numerical results for a 4 cm diameter crystal at solidified distance 6.3 cm

Concave shape of the crystal tail

Temperatures and velocities

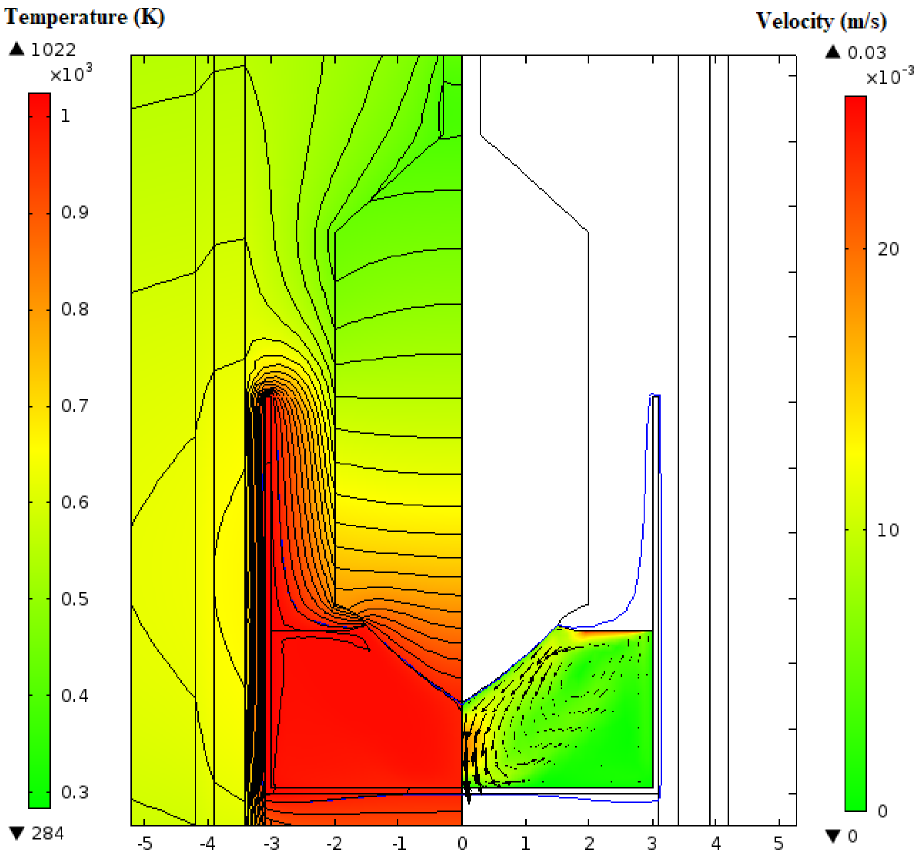

Von Mises stress

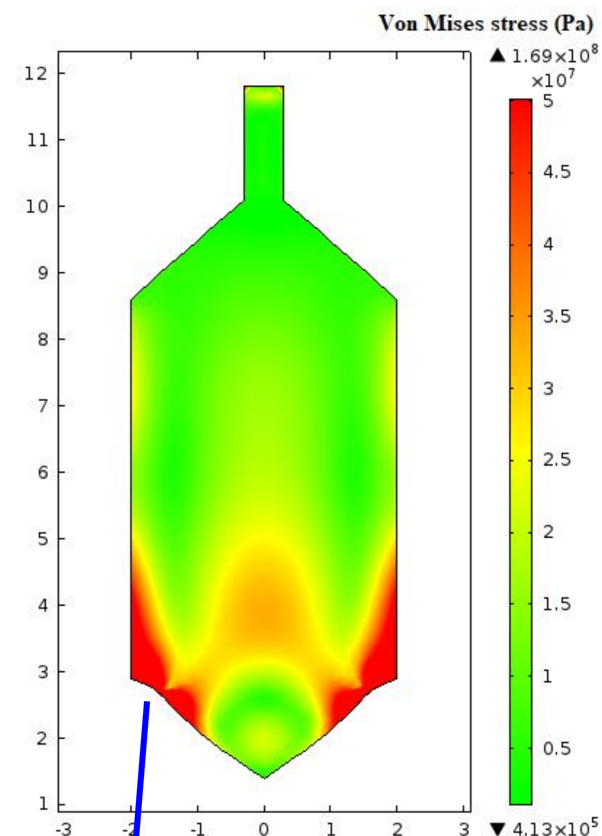

Concave shape

Numerical computations of the Von Mises stress in LMO crystal (4)

Numerical results for a 4 cm diameter crystal at solidified distance 6.3 cm

Convex shape of the crystal tail

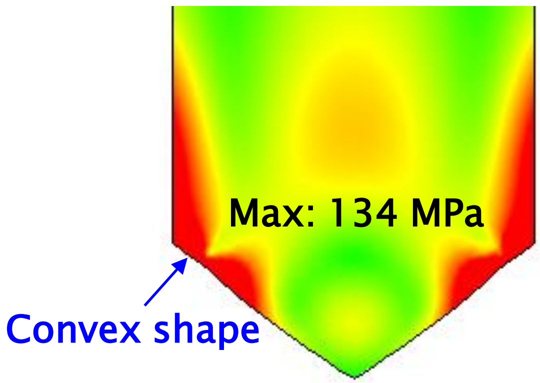

Concave shape of the crystal tail

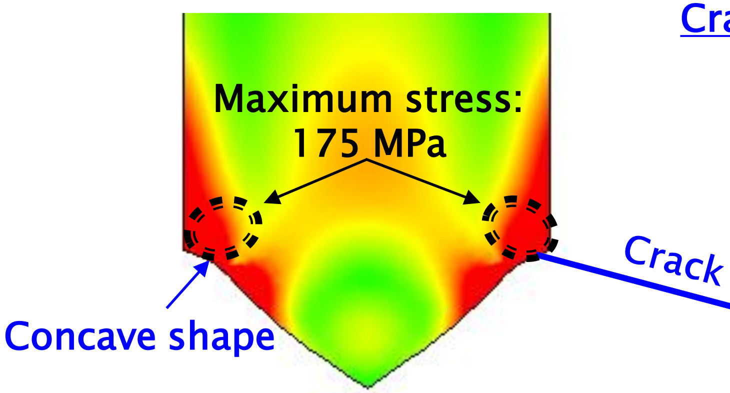

Crack formation at the bottom part of the crystal

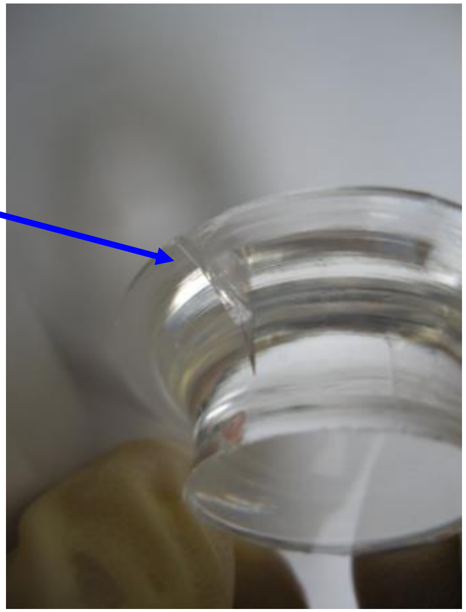

Stress distribution at the outer surface of the crystal

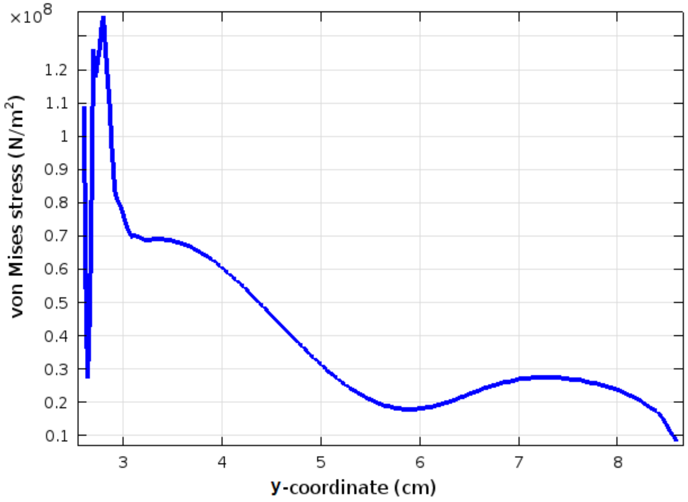

Stress distribution at the outer surface of the crystal

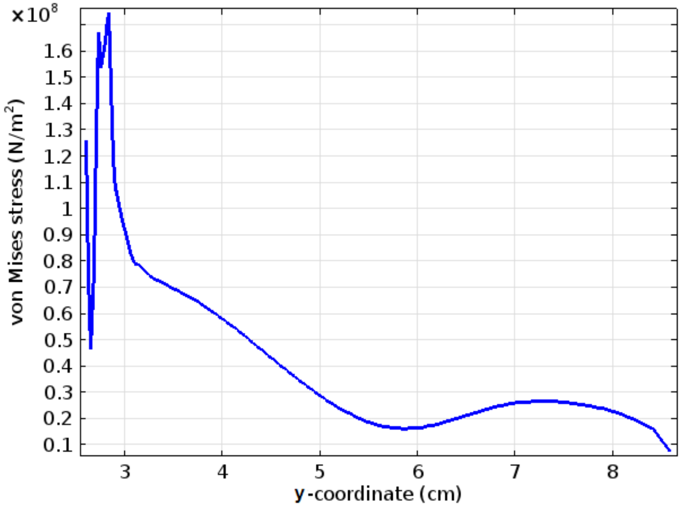

Von Mises stress increases by 30% in the case of a concave shape of the crystal tail

Stelian *et al.*, J. Cryst. Growth, 531 (2020) 125385

Numerical computations of the Von Mises stress in LMO crystal (5)

Numerical results for a 4 cm diameter crystal at solidified distance 6.3 cm with a *concave* shape of the crystal's tail

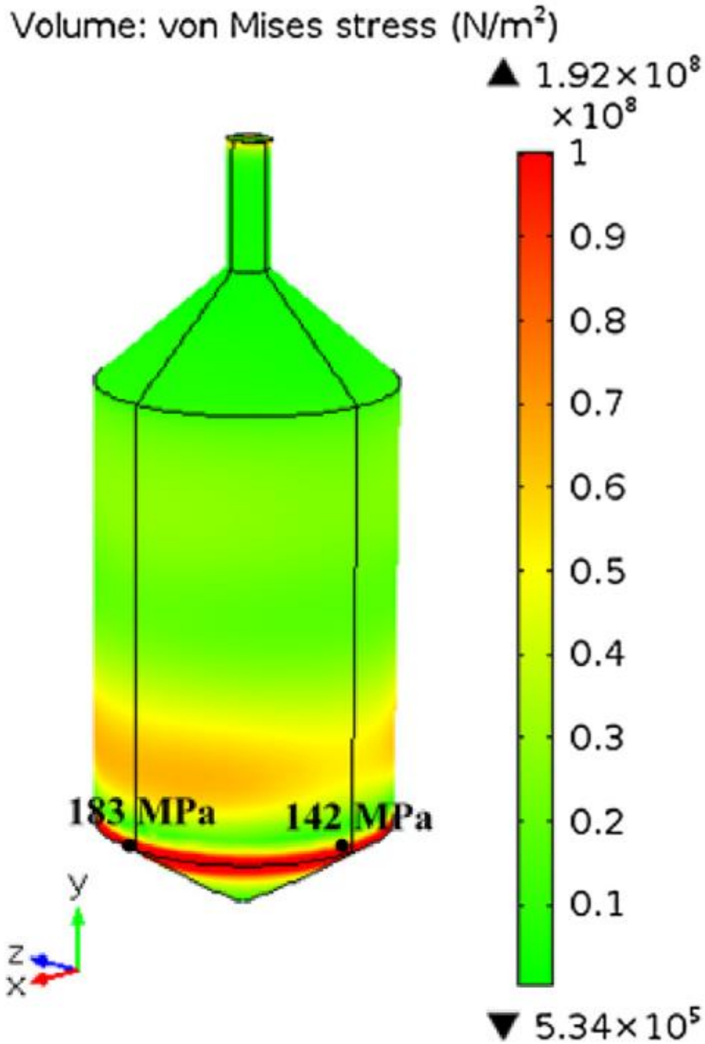

Stress distribution at the outer surface of the crystal

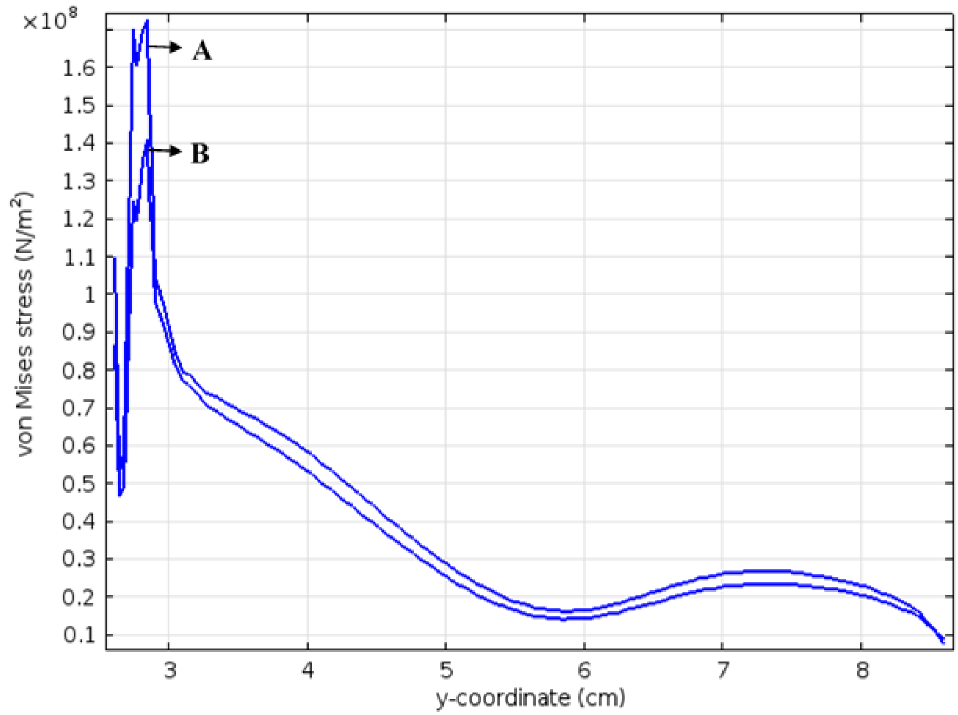

Stelian *et al.*, J. Cryst. Growth, 531 (2020) 125385

Outline

- Growth of Li_2MoO_4 (LMO) crystals by the unoptimized Czochralski method/Crack formation and characterization

- Modelling and numerical simulation of the LMO crystals Czochralski growth

- Bolometric operation with and without crystal fracture

- Absorption and scintillation emission properties of LMO crystals

- Optimized Czochralski growth of LMO crystals, thermo-mechanical properties characterizations and re-investigation of the thermal stresses

Conclusions and perspectives

HSCB operation of the cracked and uncracked Li_2MoO_4 crystals

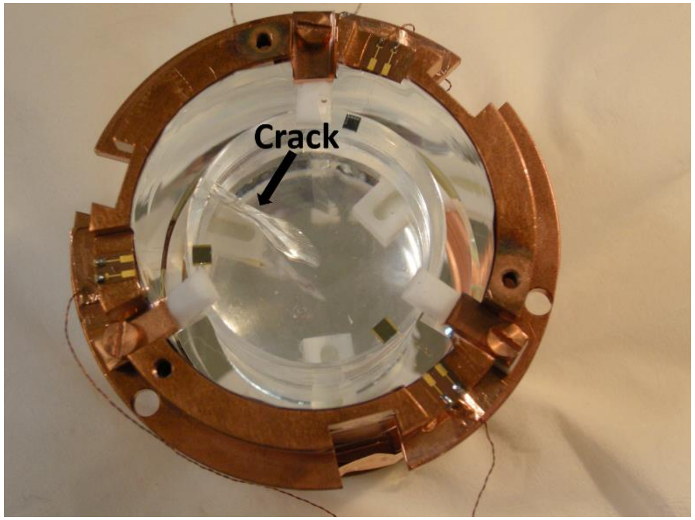

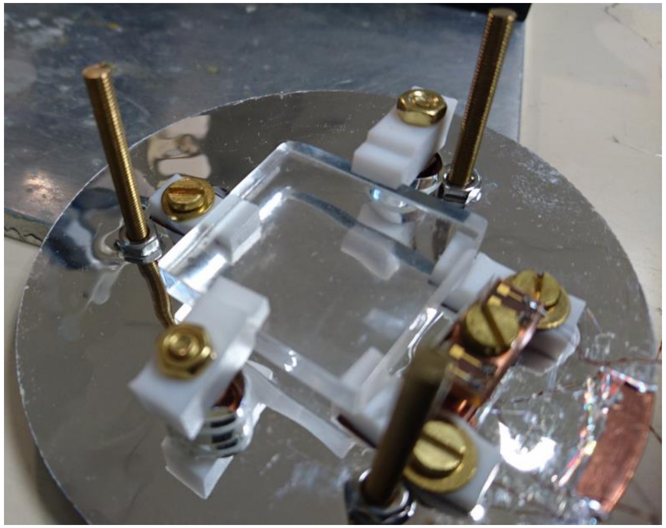

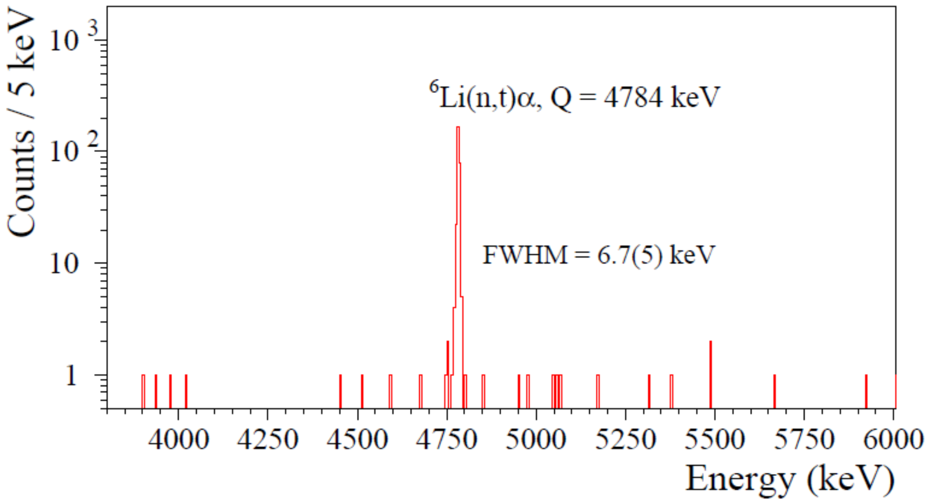

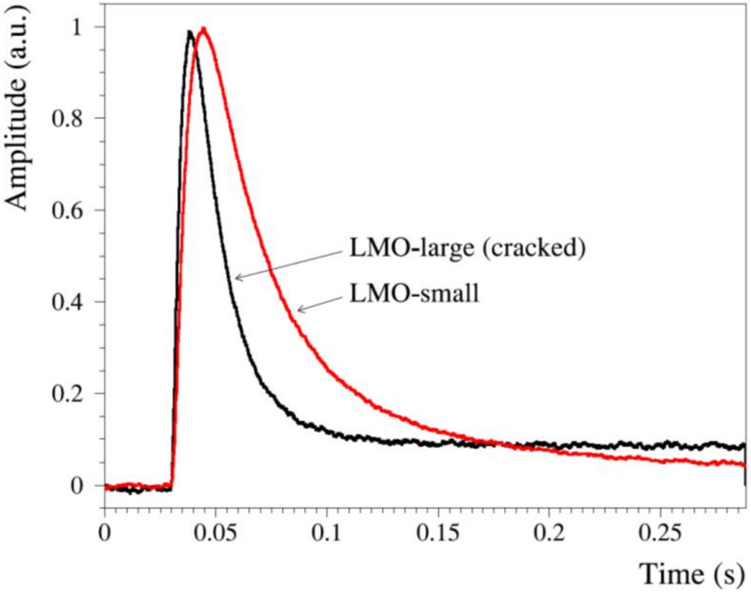

- The crack leads to a shorter response time and a second time constant of several hundreds of ms.
- Resolution ≈0.14% @ 4.8 MeV

Heat-light diagram at 20 mK of the cracked and uncracked Li_2MoO_4 crystals

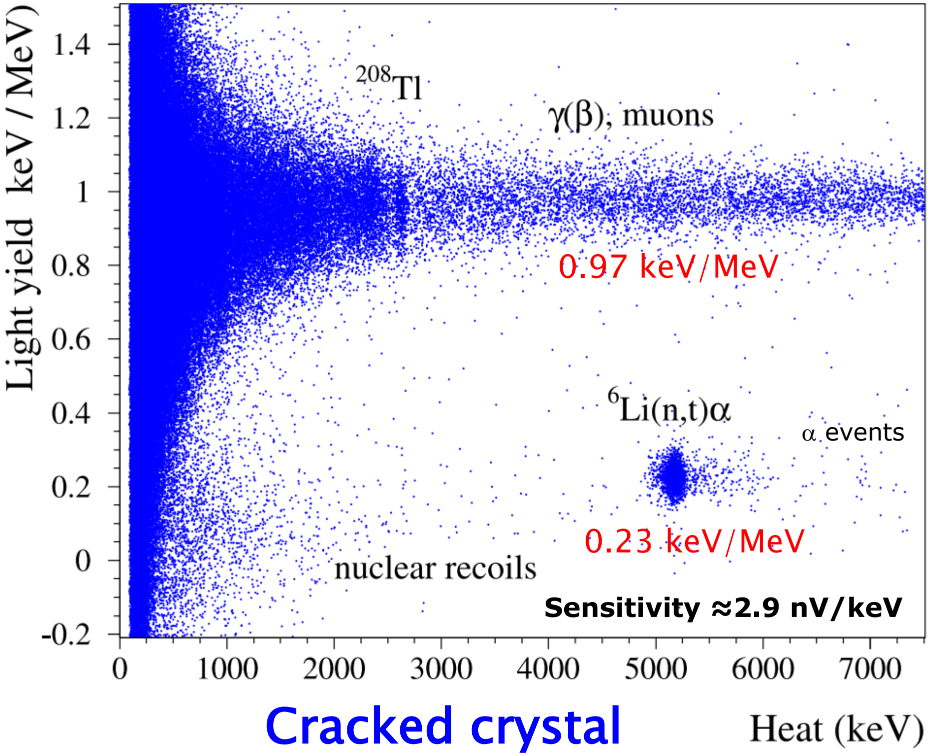

Cracked crystal

G. Buşe *et al.*, NIM A, 891 (2018) 87-91

Uncracked crystal

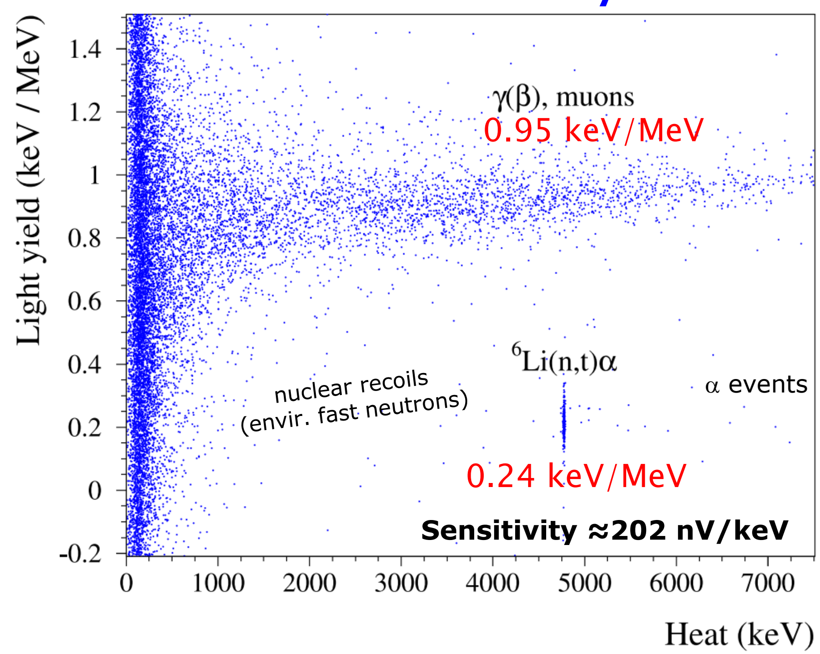

- FWHM resolution 6.7 keV @4.8 MeV in the uncracked LMO crystal, *versus* 113 keV in the cracked one (×17), and sensitivity ×70 ;
- Radiopurity levels: ^{40}K≤47 mBq/kg, ^{226}Ra≤0.37 mBq/kg, ^{232}Th≤0.21 mBq/kg, ^{228}Th≤0.27 mBq/kg.

Scintillation light yield comparison between LTG-Cz and normal Cz grown crystals

250-300 *vs* 40→28 ppm W

- CUPID-Mo meeting 2019 : 0.7 keV/MeV (^{100}Mo-enriched crystals)

- E. Armengaud *et al.*, Eur. Phys. J. C, 77 (2017) 785/1-25 :

  LMO-1 0.68 $\gamma(\beta)$ and 0.16 α
  LMO-2 0.99 and 0.20
  LMO-3 0.12 and 0.02
  ^{100}Mo-enriched LMO-B 0.77 and 0.15

- T. B. Bekker *et al.*, Astroparticle Physics, 72 (2016) 38-45 : LMO 0.7 and 0.17
- Current CUPID specification : 0.3 keV/MeV

- G. Buşe *et al.*, Nucl. Instrum. Meth. Phys. Res. A, 891 (2018) 87-91 :

  LMO-large 0.973 (~1300 ph/MeV) and α 0.2
  LMO-small 0.914 and α 0.2

☞ W- and Zn-purest LMO crystals grown to date, leading to the **highest scintillation yield ever measured in « natural » LMO crystals (≈0.97 keV/MeV, ~1300 ph/MeV).**

Outline

- Growth of Li_2MoO_4 (LMO) crystals by the unoptimized Czochralski method/Crack formation and characterization
- Modelling and numerical simulation of the LMO crystals Czochralski growth
- Bolometric operation with and without crystal fracture
- Absorption and scintillation emission properties of LMO crystals
- Optimized Czochralski growth of LMO crystals, thermo-mechanical properties characterizations and re-investigation of the thermal stresses

Conclusions and perspectives

Li_2MoO_4 optical absorption coefficient at RT

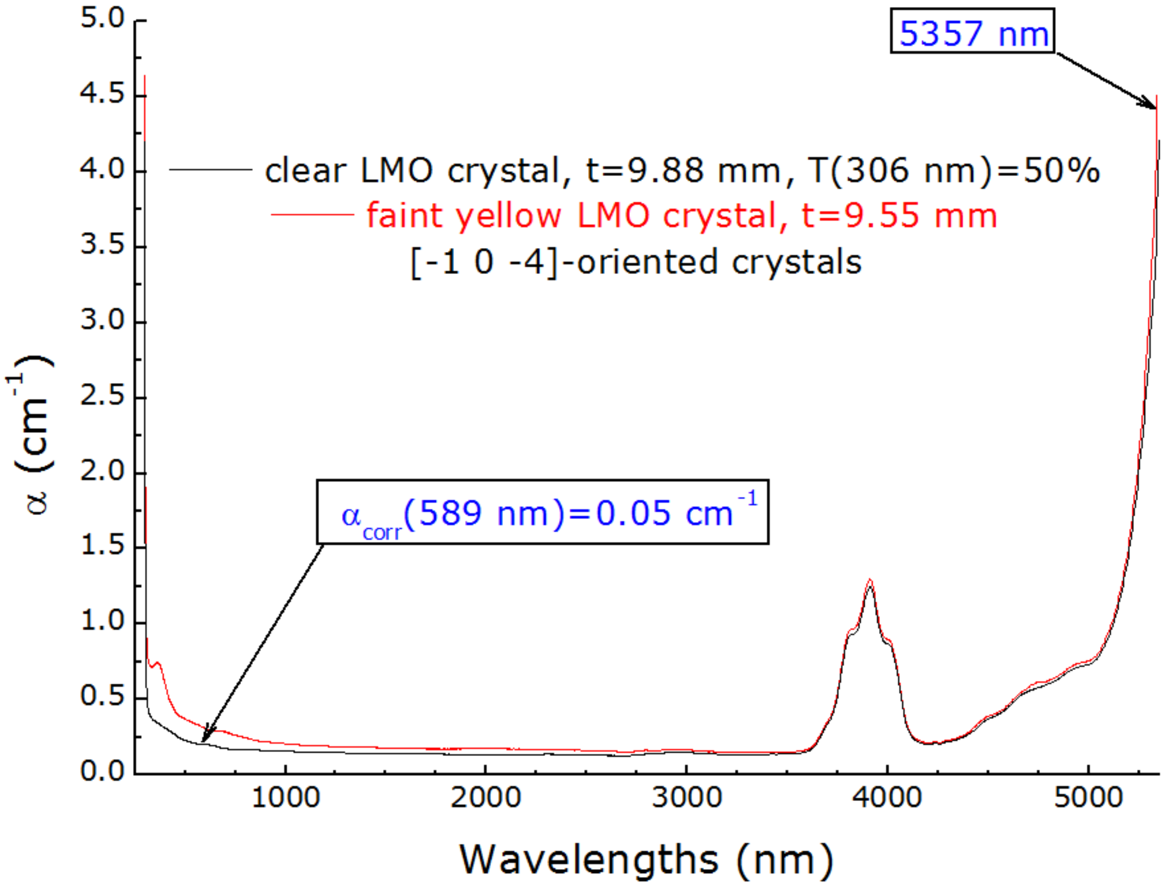

No W, Ti, Na, Fe, nor any other element found in the 10–100 ppm range by EPMA/WDS

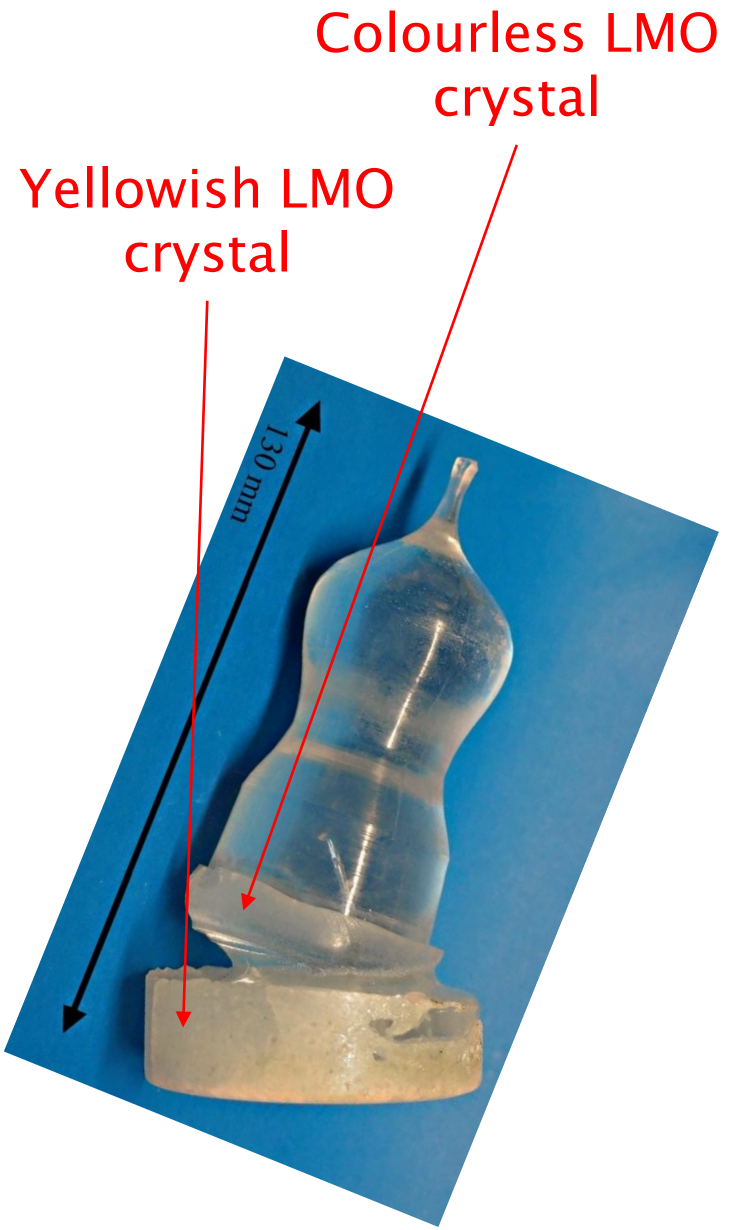

Scintillation and thermoluminescence properties of $^7Li_2MoO_4$ crystals

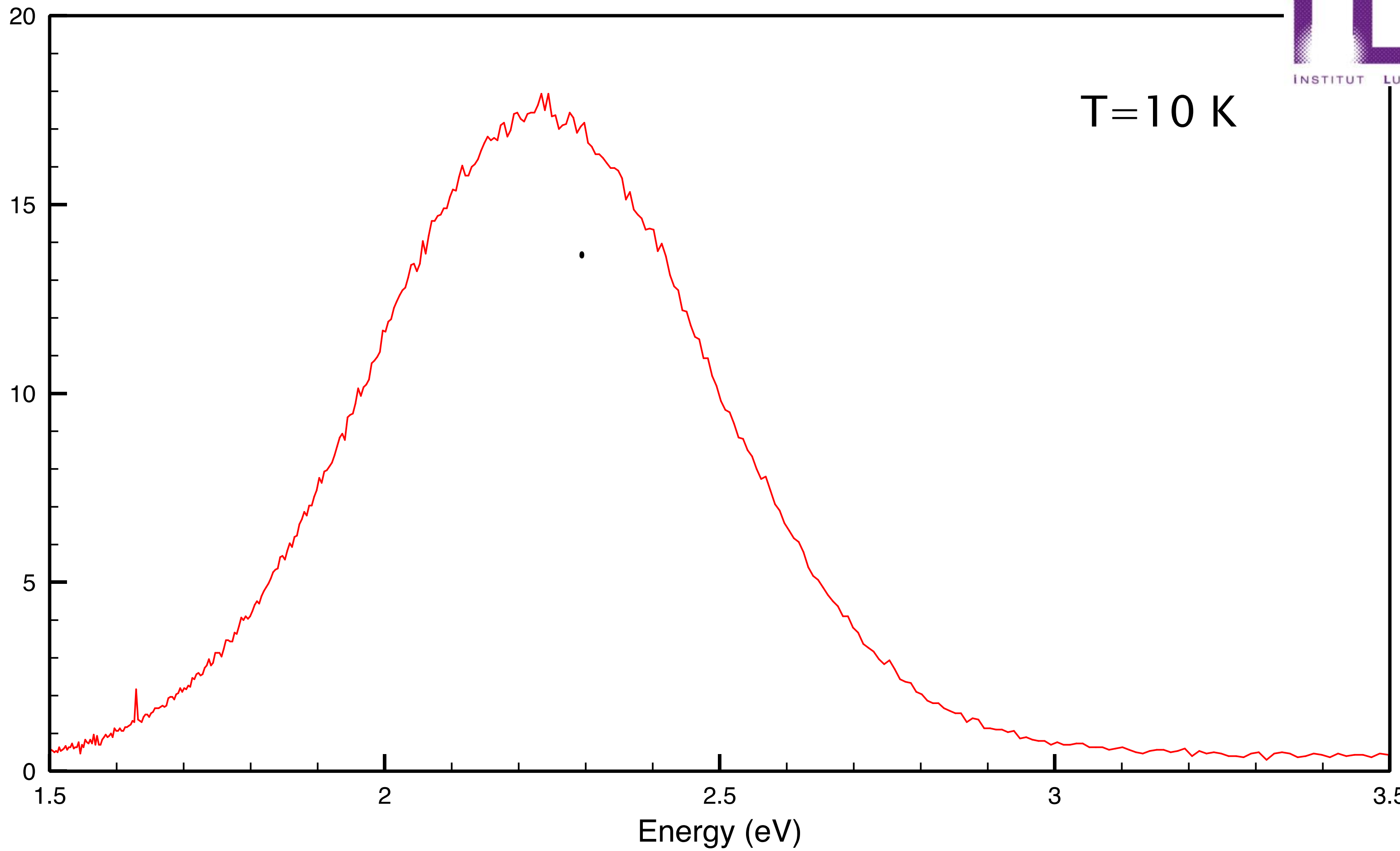

- a- T→10 K, b- X-ray excitation with W anticathode 20 mA, 20 kV, 20 mn ;
- broad scintillation band, green-yellow centered peak.

Scintillation and thermoluminescence properties of $^7Li_2MoO_4$ crystals

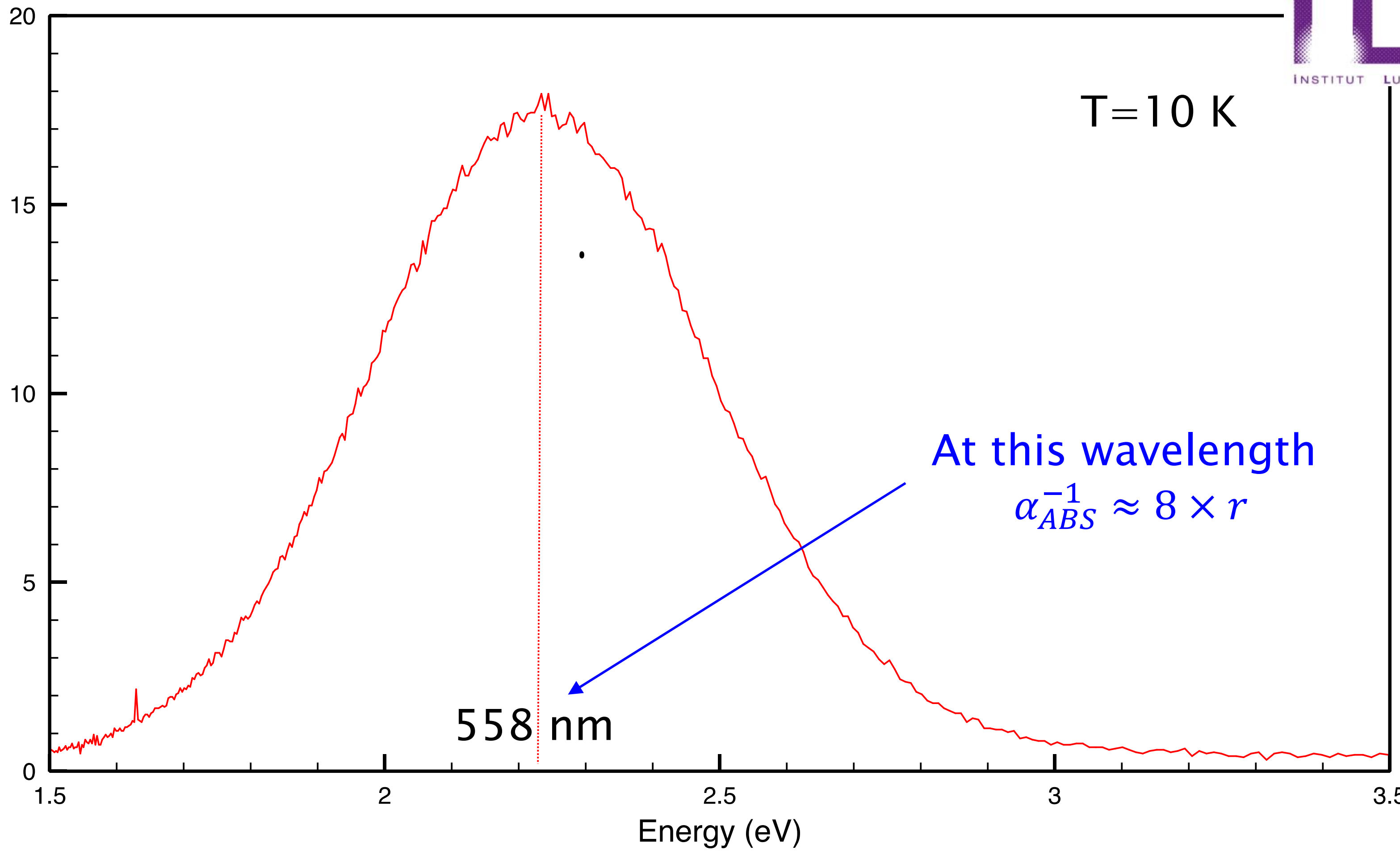

- a- T→10 K, b- X-ray excitation with W anticathode 20 mA, 20 kV, 20 mn ;
- broad scintillation band, green-yellow centered peak.

Scintillation and thermoluminescence properties of $^7Li_2MoO_4$ crystals (2)

T–λ TSL contour plot

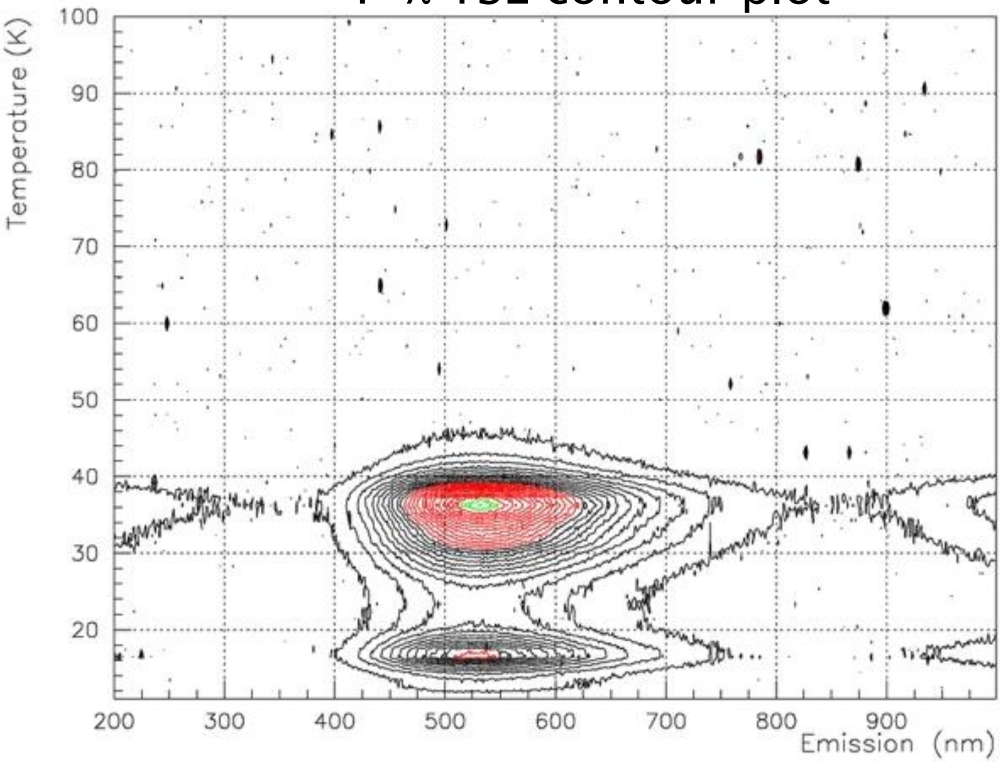

- a- T→10 K, b- X-ray excitation with W anticathode 20 mA, 20 kV, 20 mn, c- dT/dt=+6 K/mn.

Scintillation and thermoluminescence properties of $^{7}Li_2MoO_4$ crystals (2)

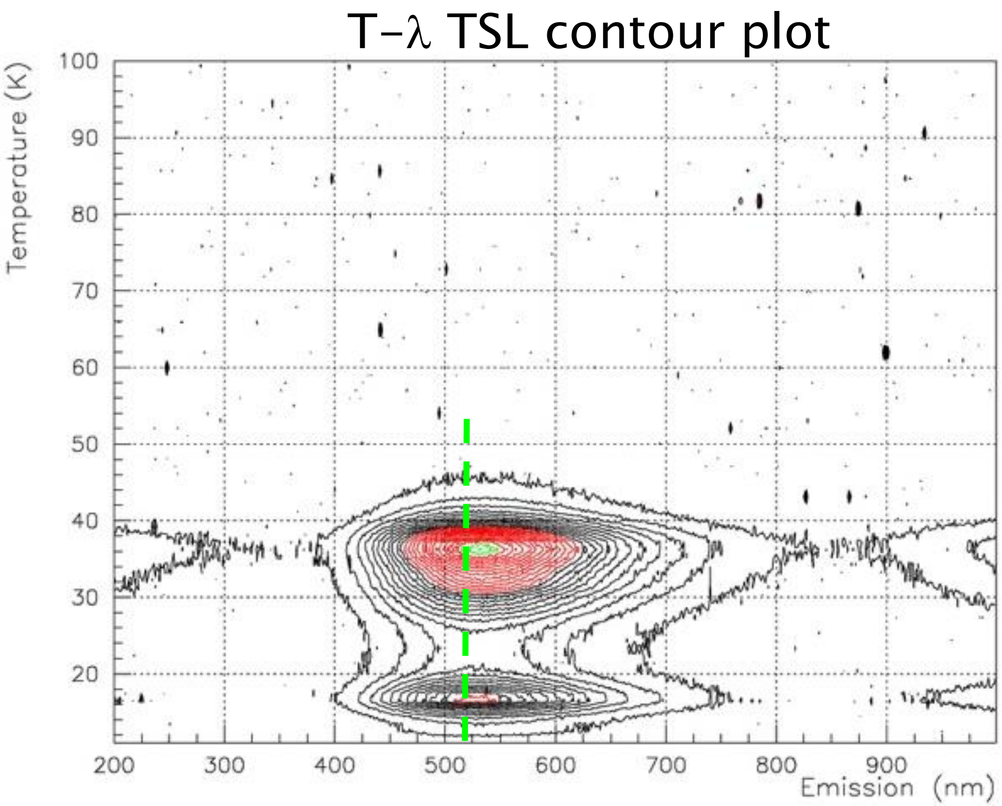

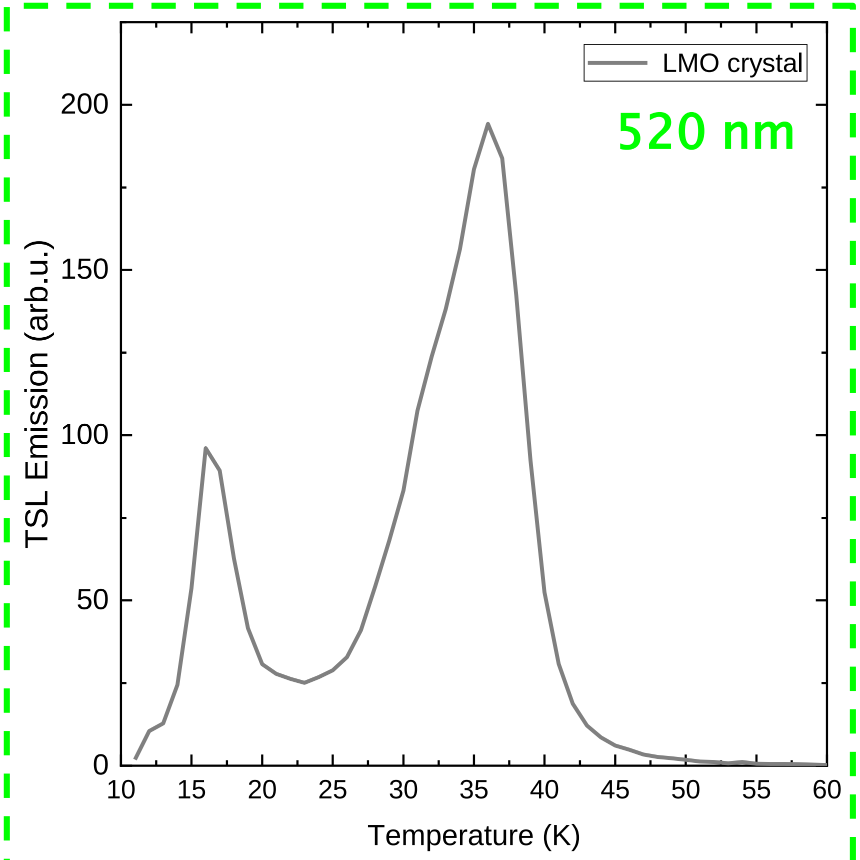

- a- T→10 K, b- X-ray excitation with W anticathode 20 mA, 20 kV, 20 mn, c- dT/dt=+6 K/mn.

Scintillation and thermoluminescence properties of $^{7}Li_2MoO_4$ crystals (2)

T-λ TSL contour plot

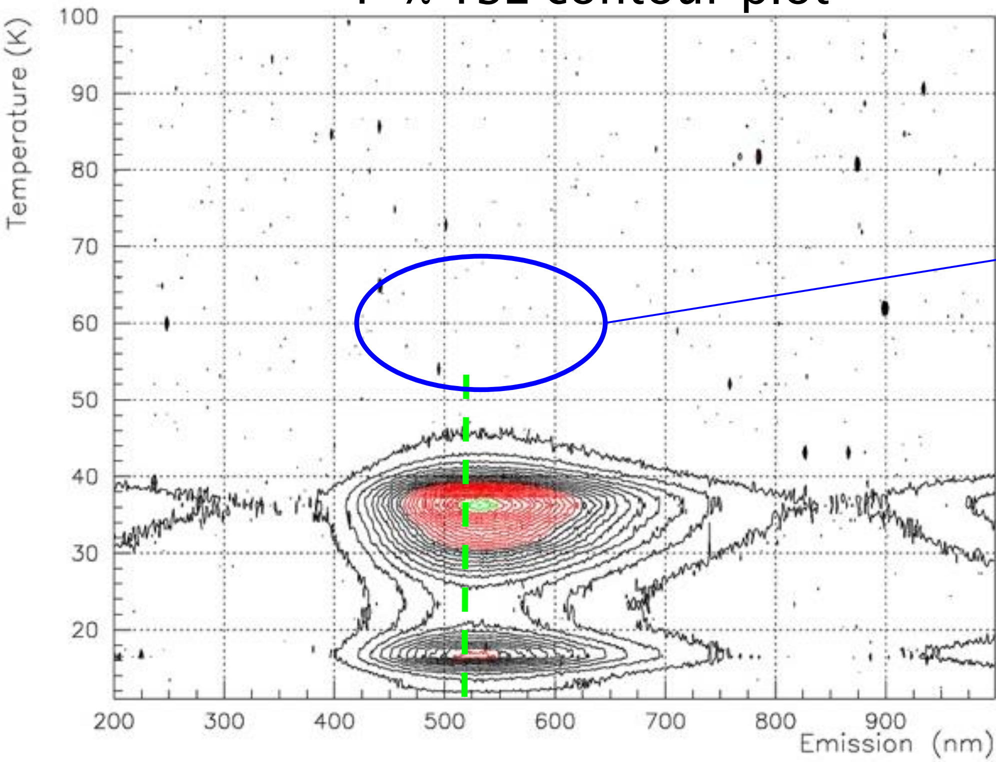

No contribution at 58 K from $Zn_{Li}^{\circ}+V_{Li}'$ point defects, as observed in LTG-Cz grown LMO crystals (Spassky *et al.*, J. Lumin. 166 (2015) 195-202)

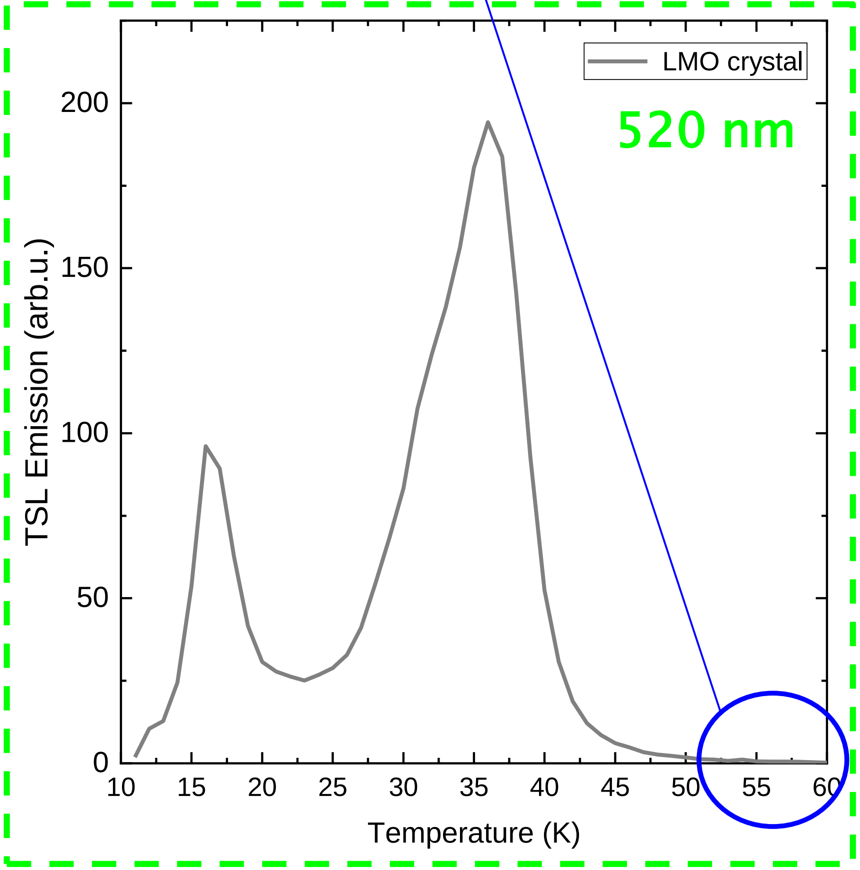

- a- T→10 K, b- X-ray excitation with W anticathode 20 mA, 20 kV, 20 mn, c- dT/dt=+6 K/mn.

Outline

- Growth of Li_2MoO_4 (LMO) crystals by the unoptimized Czochralski method/Crack formation and characterization

- Modelling and numerical simulation of the LMO crystals Czochralski growth

- Bolometric operation with and without crystal fracture

- Absorption and scintillation emission properties of LMO crystals

- Optimized Czochralski growth of LMO crystals, thermo-mechanical properties characterizations and re-investigation of the thermal stresses

Conclusions and perspectives

New chemistry laboratory in SIMaP

Linksium
technology transfer & startup building
Grenoble Alpes

PULMO project

La Région
Auvergne-Rhône-Alpes

TIRELIRE project

PhD position opening ≥ sept 2022

Optimized thermal configuration for LMO Czochralski growth

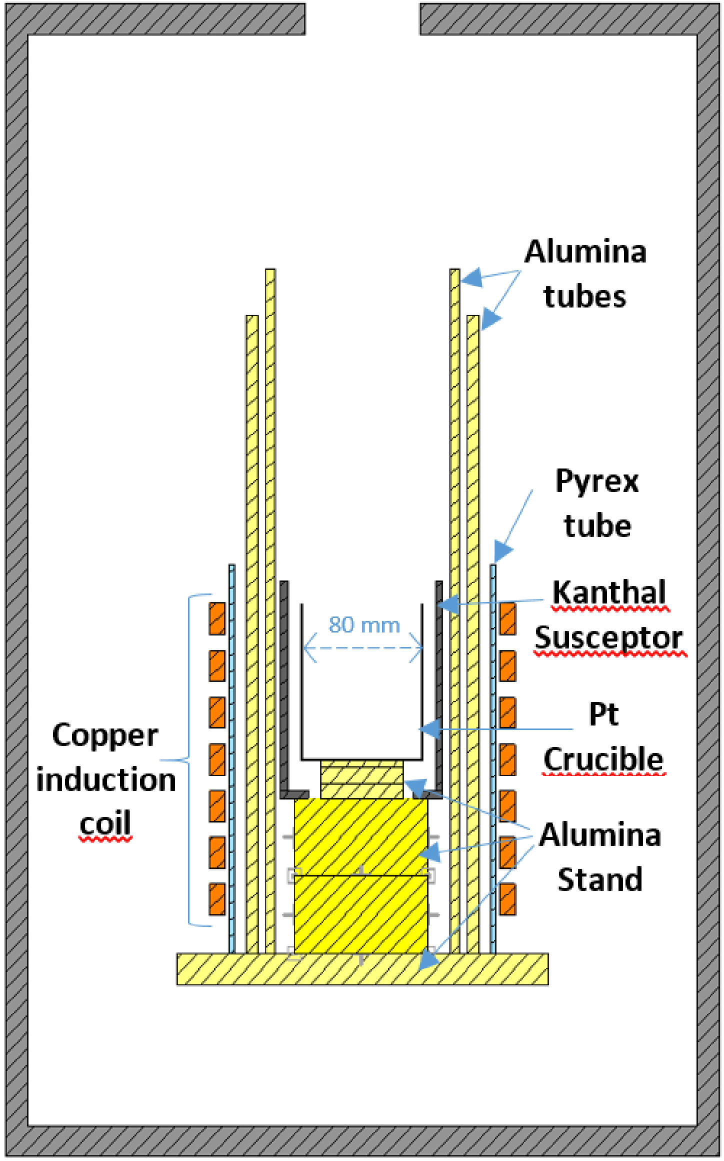

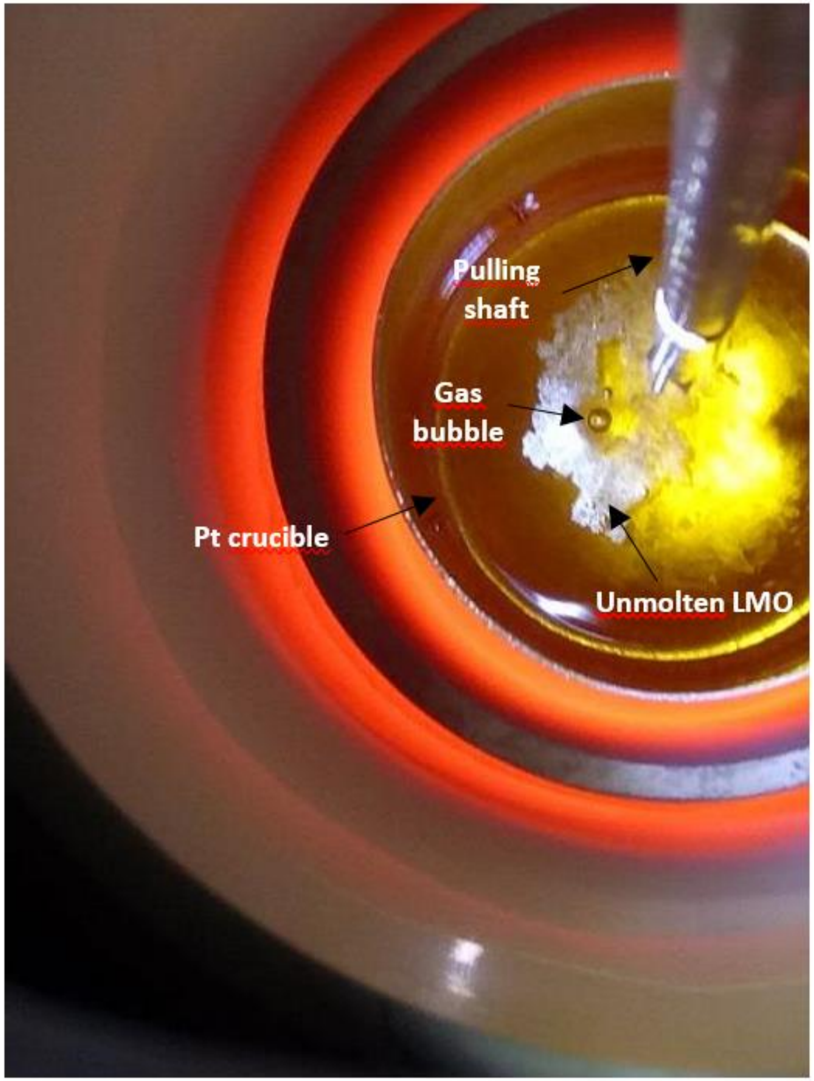

ω_{rot} = 5 rpm, v_{pull}=2 mm/h

Ahmine *et al.*, J. Cryst. Growth 15 (2022) 126420

Towards consistent kg-mass LMO crystal growth

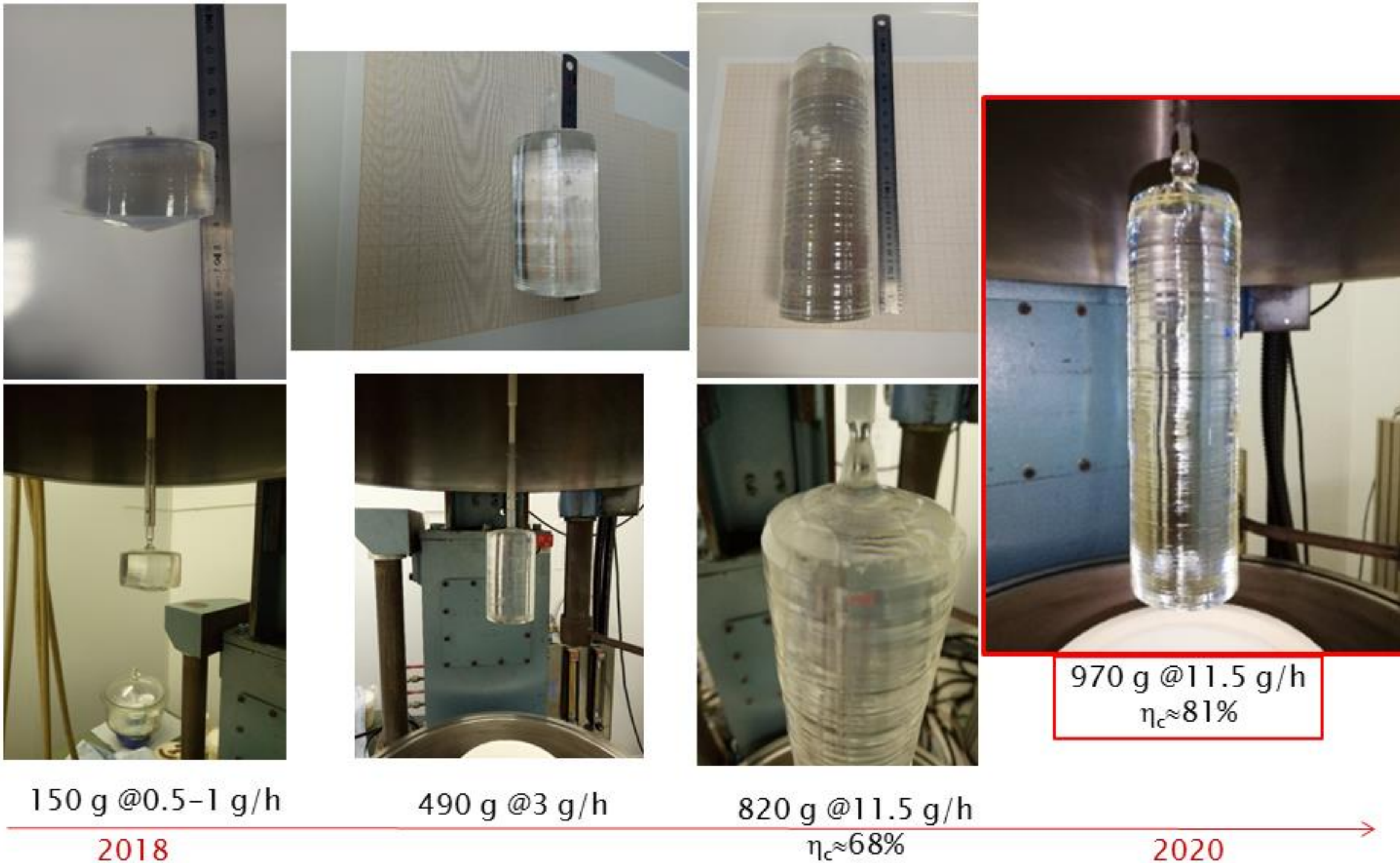

Etch pit densities measurements on oriented crystal faces

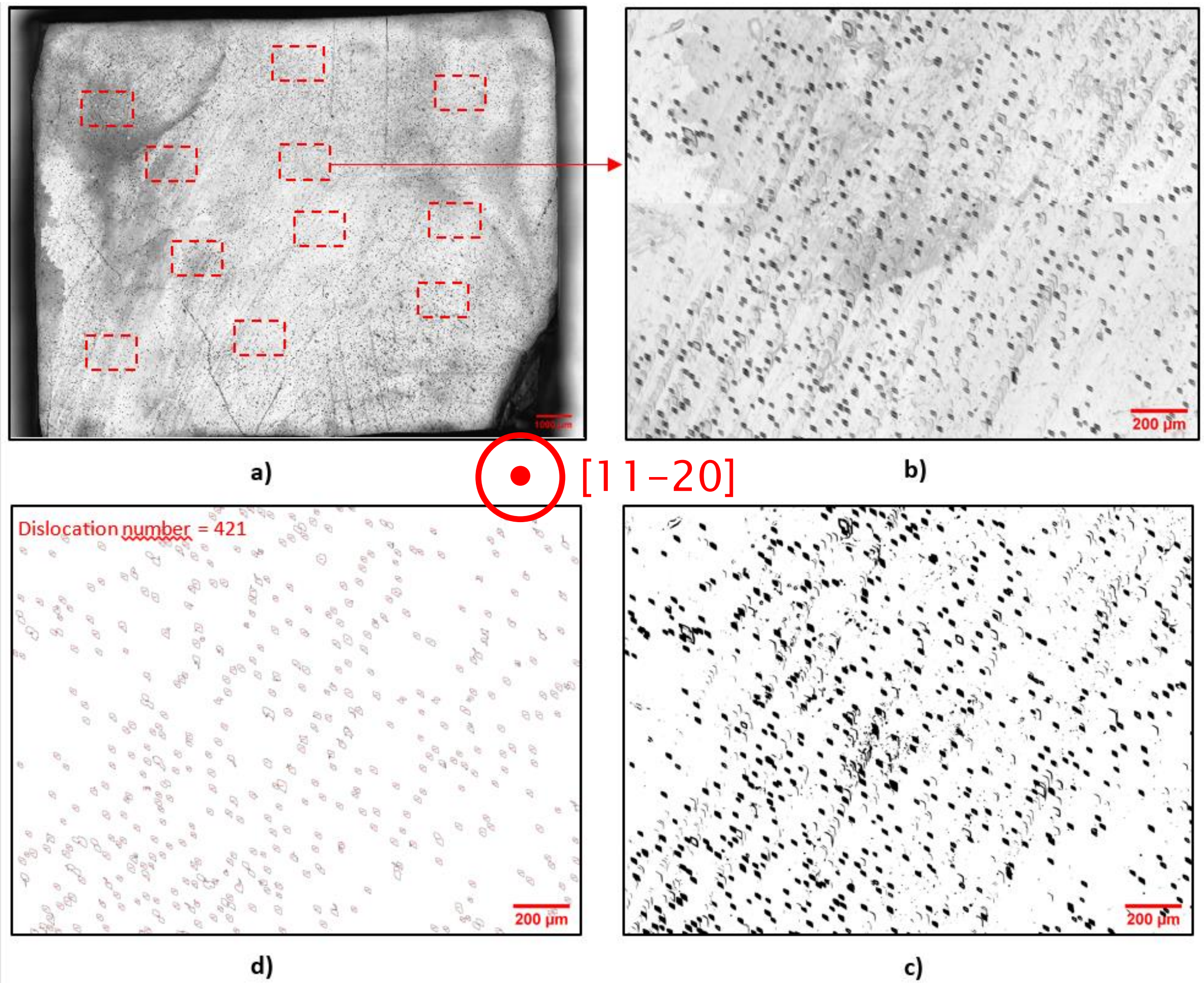

☞ In ∅=5 cm crystals, $d=(0.8 - 1.4) \times 10^4$ cm^{-2}

Ahmine *et al.*, J. Cryst. Growth 15 (2022) 126420

Etch pit densities measurements on oriented crystal faces (2)

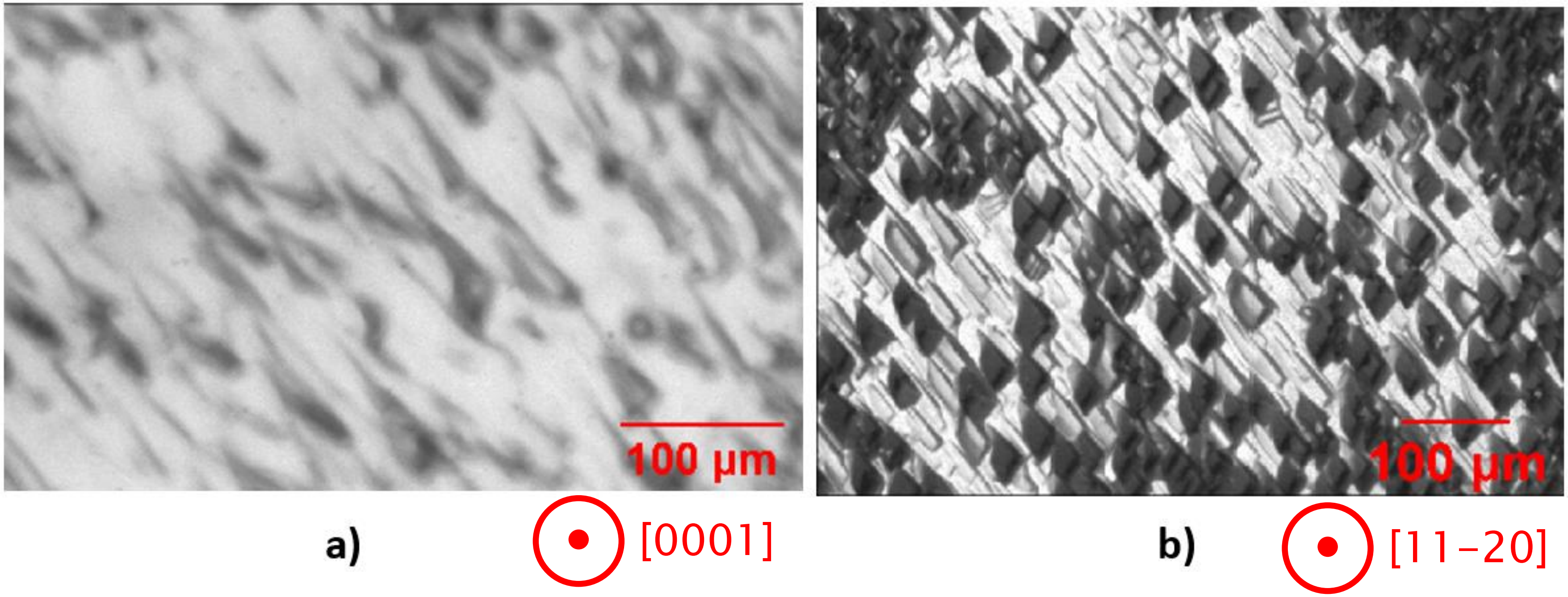

☞ Dislocations are oriented along the [11-20]-direction and contained in the (0001)-planes:
a most common slip system in rhombohedral crystals

Ahmine *et al.*, J. Cryst. Growth 15 (2022) 126420

C_{ij}–tensor measurement as a function of temperature by Brillouin spectroscopy

- Li_2MoO_4, R–3, 7 independent elements, but C_{14} and $C_{15} \approx C_{ij}/(20–100)$

$$C_{ij} = \begin{pmatrix} c_{11} & c_{12} & c_{13} & c_{14} & -c_{15} & 0 \\ c_{12} & c_{11} & c_{13} & -c_{14} & c_{15} & 0 \\ c_{13} & c_{13} & c_{33} & 0 & 0 & 0 \\ c_{14} & -c_{14} & 0 & c_{44} & 0 & c_{15} \\ -c_{15} & c_{15} & 0 & 0 & c_{44} & c_{14} \\ 0 & 0 & 0 & c_{15} & c_{14} & \frac{(c_{11}-c_{12})}{2} \end{pmatrix}$$

Collaboration with P. Djémia
LSPM–CNRS, Villetaneuse
France

- B=42 GPa, E=48 GPa, G=18 GPa, ν=0.31

$$\rho\,(kg.m^{-3}) = -0.407\,T\,(K) + 3188$$

$$C_{11}(GPa) = -0{,}024\,T\,(K) + 70.6$$

$$C_{33}(GPa) = -0{,}031\,T\,(K) + 95.7$$

$$C_{13}(GPa) = -0{,}007\,T\,(K) + 26.3$$

$$C_{12}(GPa) = -0{,}016\,T\,(K) + 43.2$$

$$C_{44}(GPa) = -0{,}004\,T\,(K) + 17.3$$

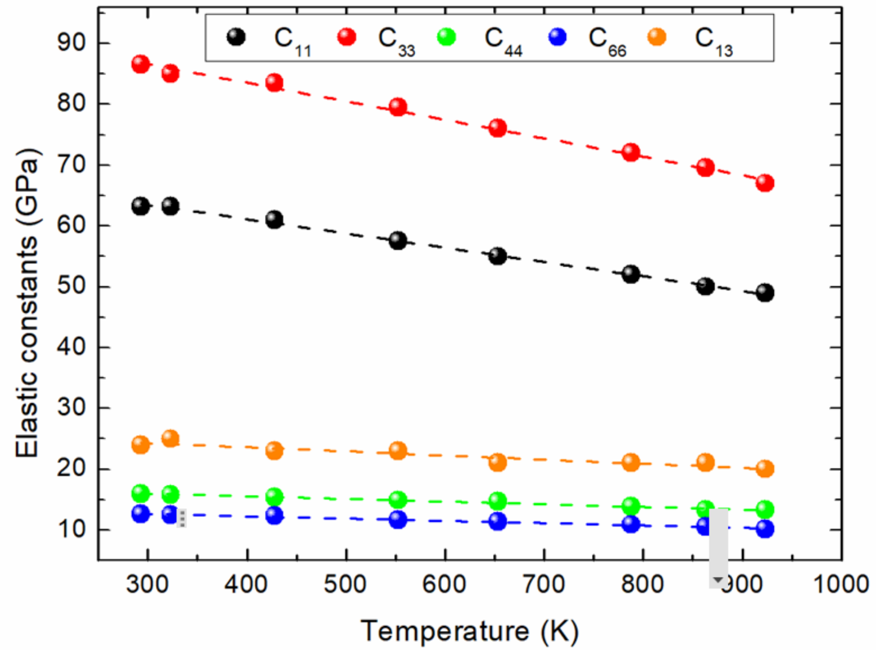

Ahmine *et al.*, submitted J. App. Phys. (2021)

Rupture uniaxial compressive tests as a function of temperature

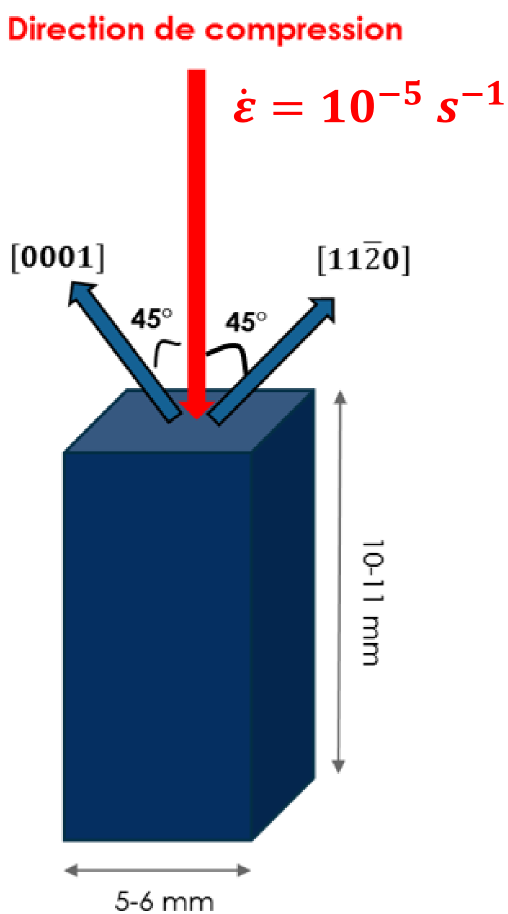

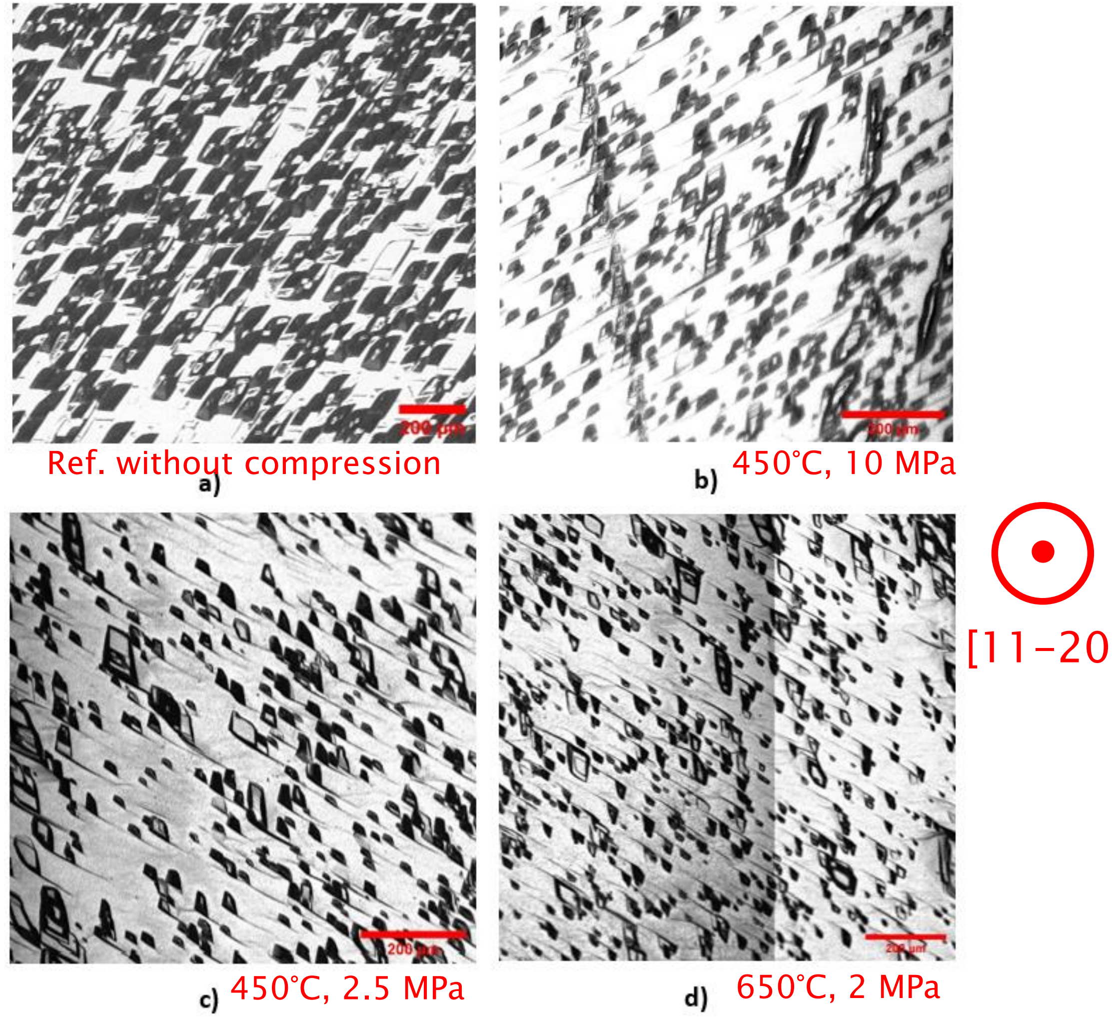

- Single crystals rupture tests in uniaxial compression @45° from both [0001] and [11-20] directions, performed at RT, 450°C and 650°C showed no significant change in dislocation concentrations, and no twinning in the fractured crystals
- Crack formation stress 7.5>σ>3 MPa @650°C

Ahmine *et al.*, submitted J. App. Phys. (2021)

Lattice parameters thermal expansion and dilatometry in Li_2MoO_4

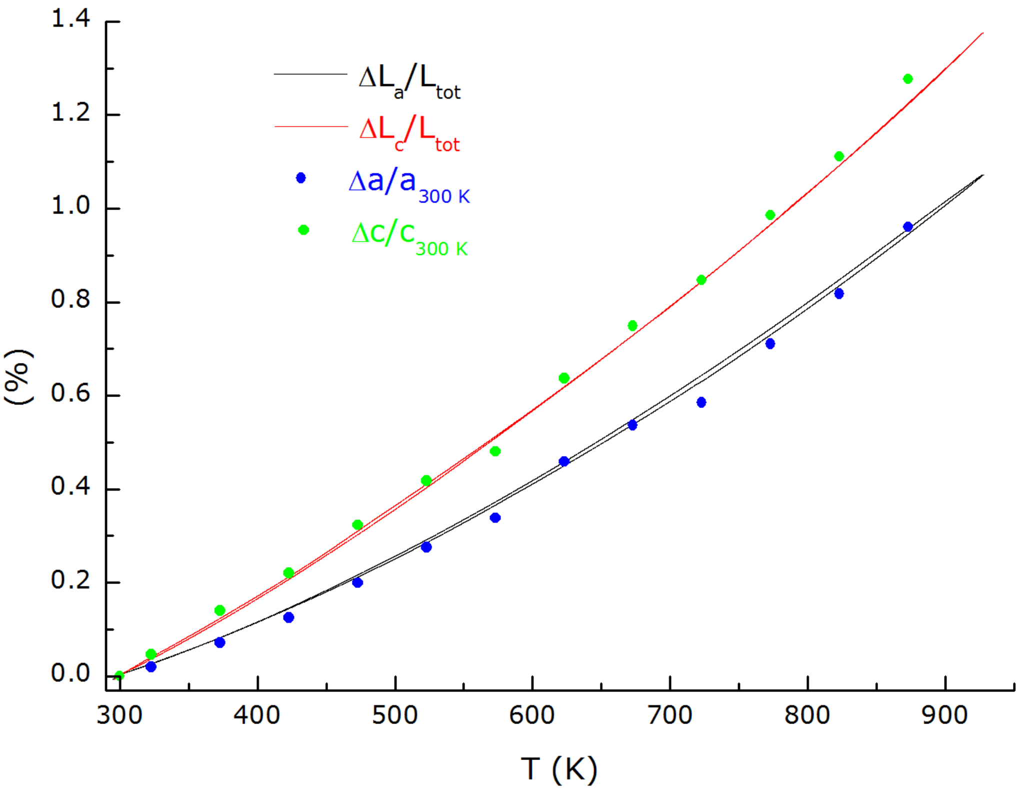

- Both curves superimpose, suggesting the absence of vacancy and interstitial formation up to $0.9T_m$, and so no plastic creep during solidification, or the formation of both point defects types mutually compensating each other, leading to a completely reversible and parabolic in temperature thermal expansion ;

- On average between 100 K and room temperature, the thermal contraction upon cooling is 1.4 times higher than in Ge.

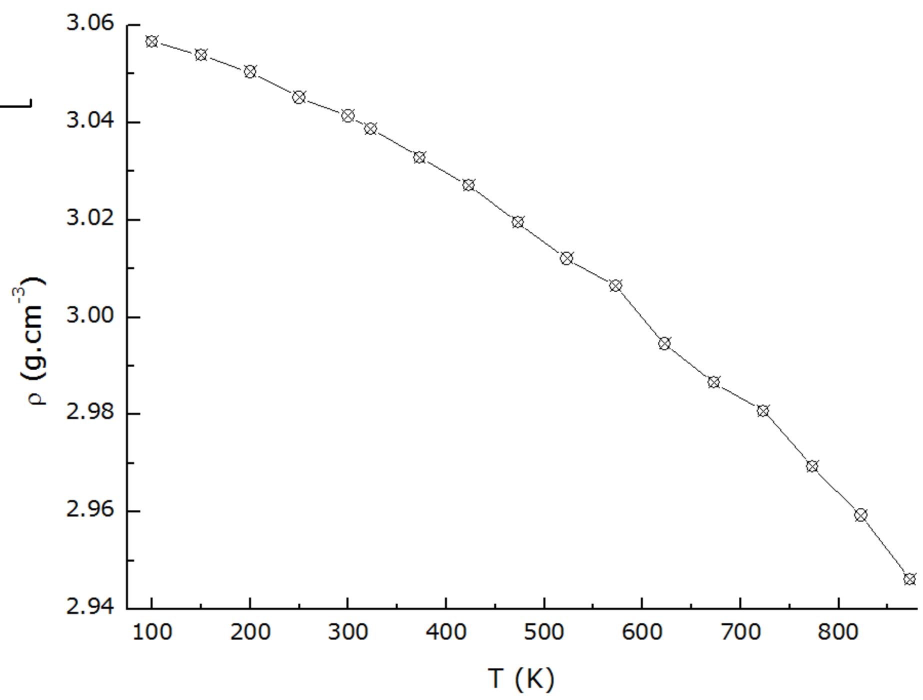

Velázquez *et al.*, Sol. St. Sci., 65 (2017) 41-51

Temperature field in the crystal and surroundings at three times during growth

$|\nabla T|_{max} = 30\ K.cm^{-1}$

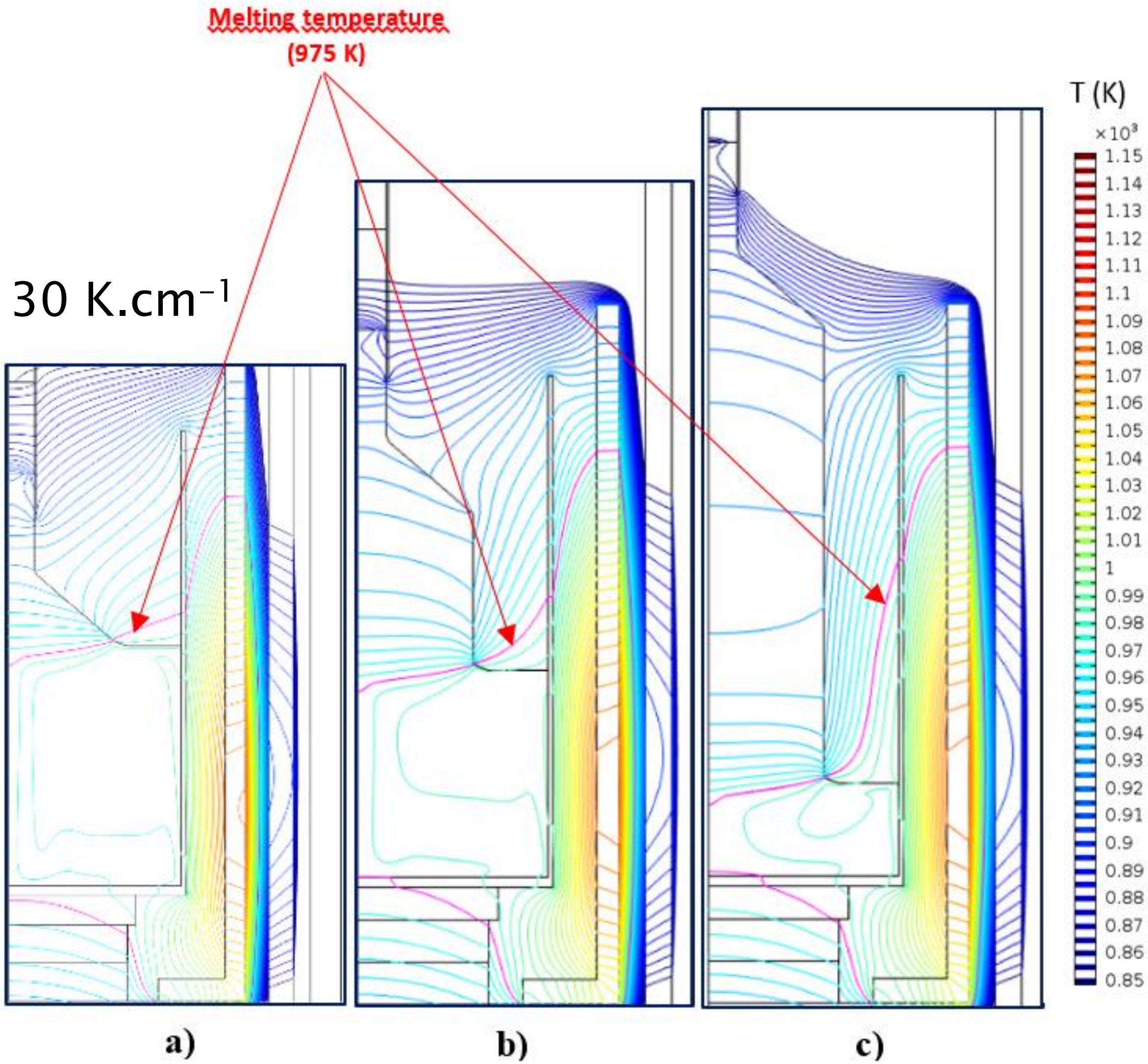

Ahmine *et al.*, J. Cryst. Growth 15 (2022) 126420

Experimental validation of the temperature field calculations

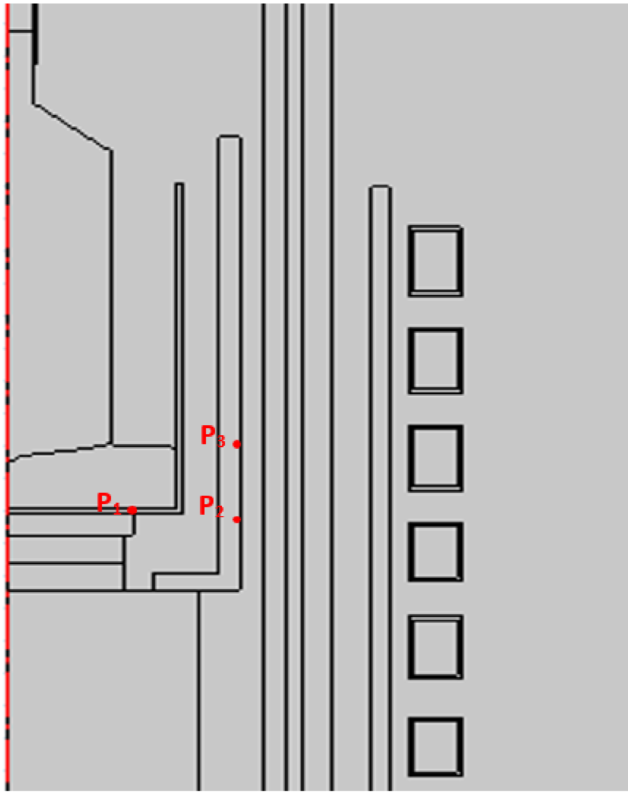

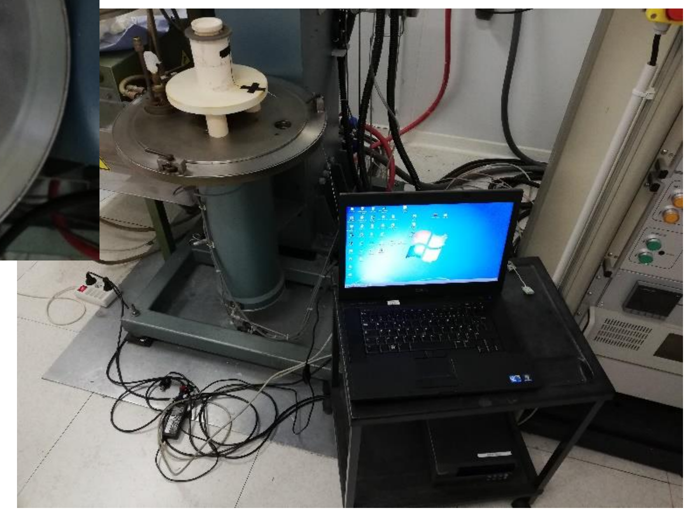

	P_1	P_2	P_3
Measured T (K)	1002	1094	1100
Calculated T (K)	984	1073	1082

- Calculated interface deflection f_{calc}~4 mm at three times during the growth, *versus* experimental deflection at the end of the growth f_{exp}=3.7 mm

Velocity field in the molten bath at three times during growth

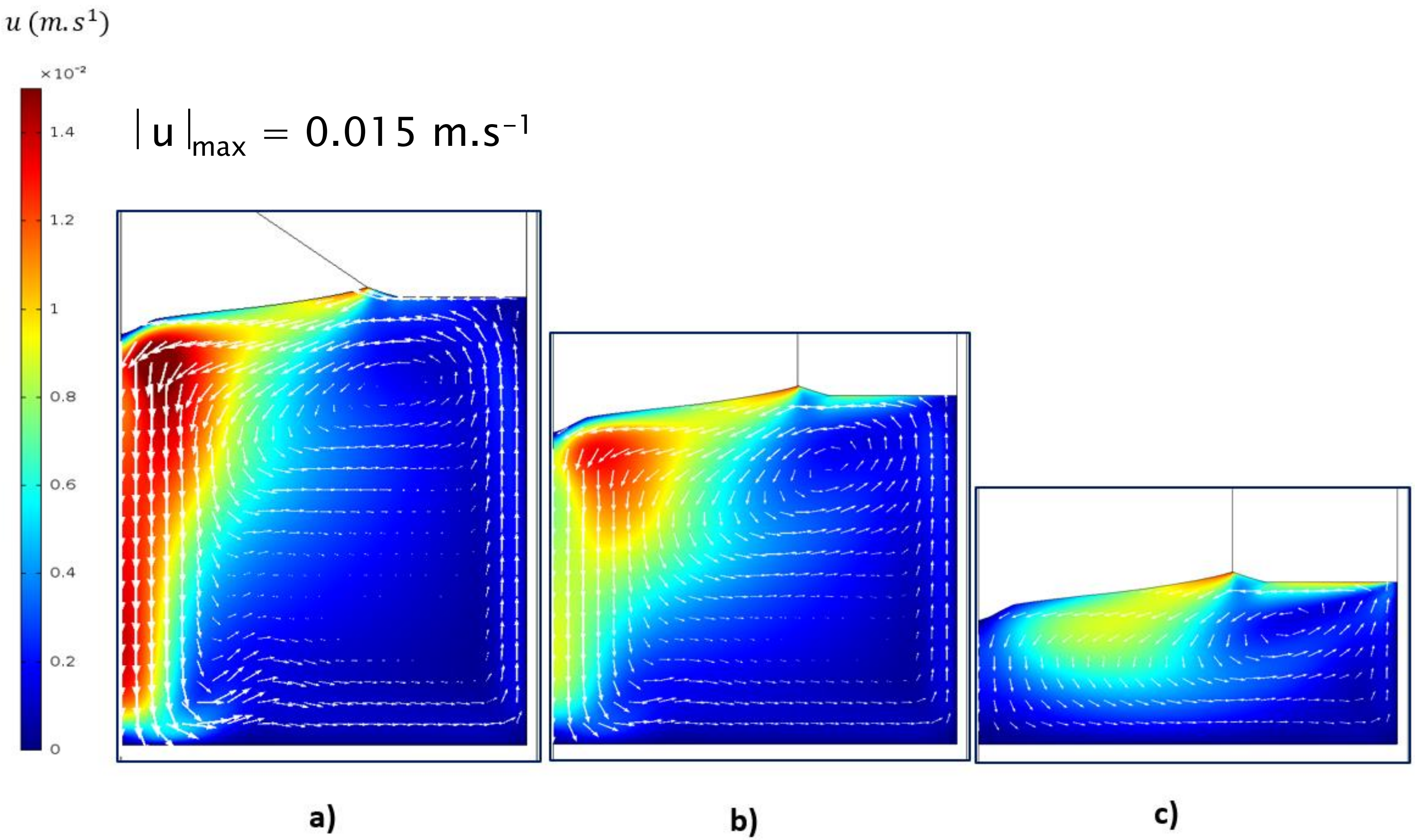

Compressive and tensile stresses during growth projected on a (0001) fracture plane

Compressive and tensile stresses during growth projected on a (0001) fracture plane

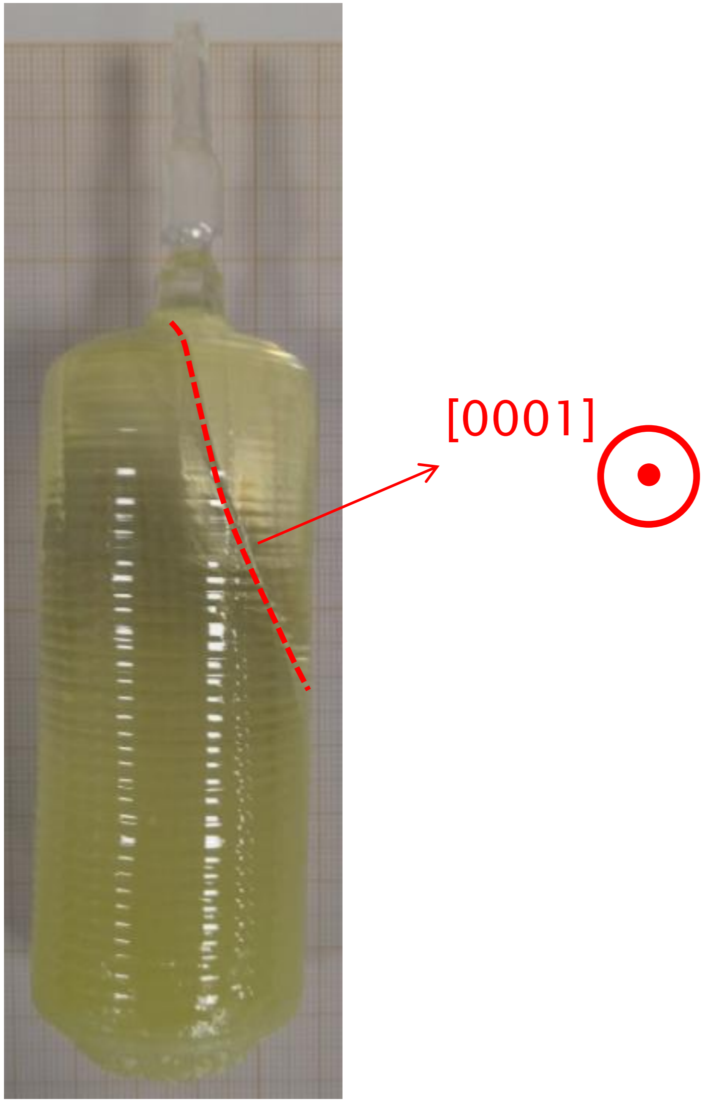

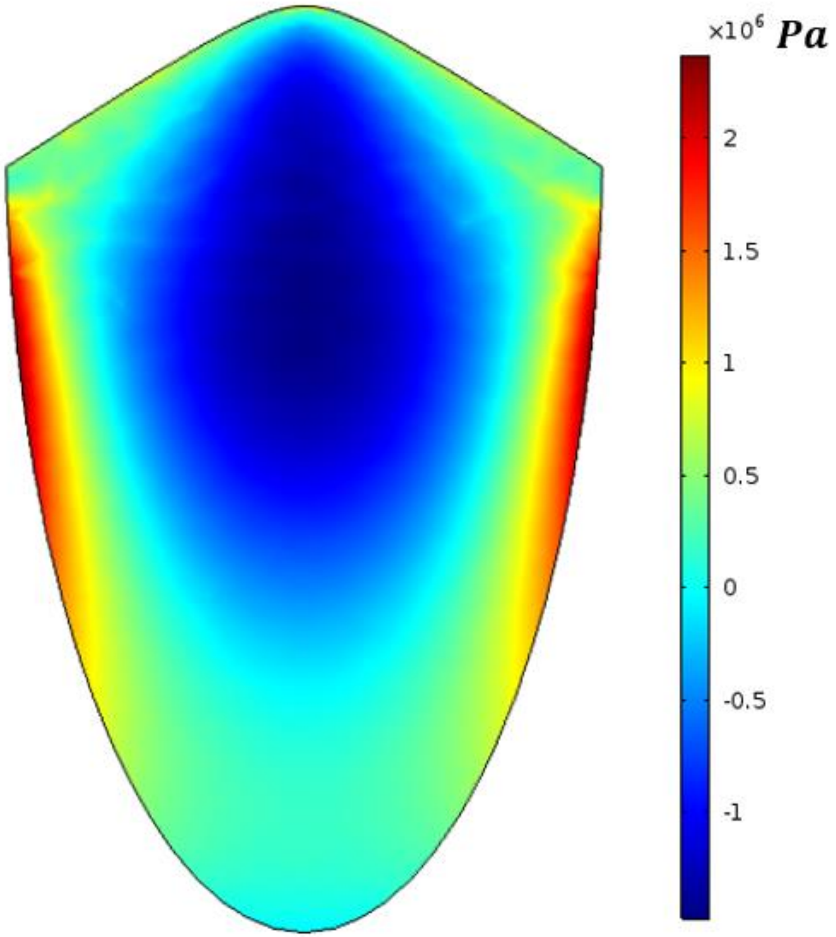

Tensile $\sigma_{max} = 2$ MPa

Ahmine *et al.*, J. Cryst. Growth 15 (2022) 126420

Conclusions and perspectives

- Elaboration and characterization of a 230 g Li_2MoO_4 single crystal's physical properties, radiopure (^{40}K<47 mBq/kg, <0.2–0.3 mBq/kg on U/Th), scintillating at very low temperature (0.97 keV/MeV on γ's), of resolution 6.7 keV @4.8 MeV and of discrimination factor $(\alpha+t)/\gamma(\beta) \approx$ 9–10 ;

- By heat-power regulation coupled to automated mass weighing, and coupling to a susceptor between the induction coil and the crucible, we managed to grow repeatedly kg-mass LMO crystals at faster pulling rates, with crystallization yields comparable to those obtained by the LTG-Cz technique, keeping the solidification isotherm stable and remote from the bottom of the crucible and the liquid-gas free surface temperature lower than 725°C ;

- We are now focusing on purifying the initial materials, Li_2CO_3 and MoO_3 powders to prepare growth charges which will be used for the growth of larger diameter crystals ($\varnothing$=6.4 cm) ;

- Characterizing and modelling the macropartition radioimpurities profiles is still a important task to do, in order to be able to optimize the recycling procedures ($^{100}Mo \approx$60–70 €/g; $^{6}Li \approx$42 €/g; $^{7}Li \approx$13 €/g).

PULMO

MATURATION

De la poudre au cœur de bolomètre : purifier pour détecter

Exporter la fiche

Contact Linksium
Stéphan Pédèche
+33 (0)6 73 17 55 36
stephan.pedeche@linksium.fr

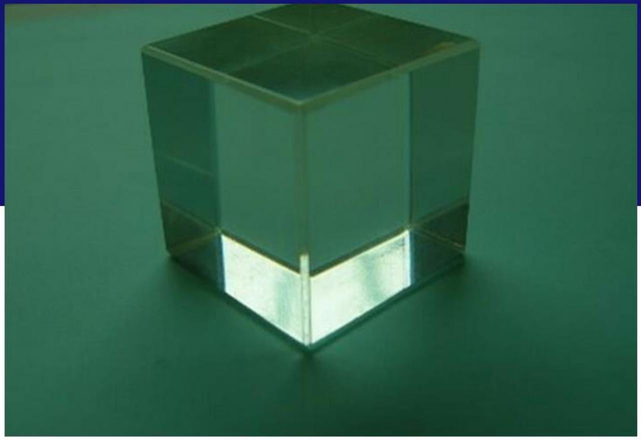

^{6}LMO crystal

Bénéfices

- Sécurisation de la filière européenne
- Reproductibilité des cristaux
- Haute qualité

Mots clefs

- Purification
- Croissance cristalline
- Recyclage
- Mise en forme

Propriété Intellectuelle

- 4 savoir-faire

Partenariats & Récompenses

- Région Auvergne-Rhône-Alpes (docTT'auRA)

Laboratoire

- SIMAP

Établissement

- CNRS

Continuum Linksium

- Maturation

Résultats

- Startups créées

Contexte

Contribution à la découverte et à la compréhension des constituants ultimes de la matière (neutralino, neutrons, neutrinos, ...) et à la souveraineté et à la résilience technologiques de l'Europe en matière de sûreté nucléaire.

Technologie

- Purification des matières premières, enrichies en isotopes extrêmement onéreux et géostratégiques, et engagées dans l'élaboration des cœurs de bolomètres cryogéniques à chaleur-scintillation déployés en détection des évènements rares.
- Élaboration de composants massifs répondant à un cahier des charges contraignant en termes de radiopureté, de forme, de transparence optique, de qualité cristalline, de rendement de scintillation, de rendement en masse d'isotope et de délais de production et de livraison.

Avantages

- Efficacité de purification mise à l'échelle avec un rendement en masse de 93% et seulement 2% de pertes de matière.
- Rapidité d'élaboration des composants monocristallins massifs avec recyclage de charge.
- Technologie de croissance à coûts réduits (équipement, refroidissement, consommation électrique).
- Protection factuelle de savoir-faire dans un domaine où l'évolution des techniques d'analyse ne permettra pas une ingénierie inverse facile.

Maturité

- Très forte demande internationale à satisfaire sur un temps court.
- Procédés de purification et de croissance à TRL3, en phase de mise à l'échelle pour un assemblage des différentes briques technologiques.

Applications

- Purification et recyclage d'isotopes extrêmement onéreux.
- Cœur monocristallins de bolomètres cryogéniques à chaleur-scintillation.
- Substrats pour procédés de dépôts de couches minces à T£650°C.

New crystal growth furnaces in SIMaP

Optical floating zone furnace (~3000°C)

Saphire, YAG, …

Czochralski furnace (~1000°C)
Under construction

Molybdates, tungstates, borates, …


Let’s build projects together !